Supporting Information

Two Isostructural URJC-4 Materials: From Hydrogen Physisorption to Heterogeneous Reductive Amination Through Hydrogen Molecule Activation at Low Pressure

Helena Montes-Andrés[⊥], Pedro Leo[⊥], Antonio Muñoz[⊥], Antonio Rodríguez-Diéguez[§], Gisela Orcajo[†], Duane Choquesillo-Lazarte[∇], Carmen Martos[†], Fernando Martínez[⊥], Juan A. Botas[†], Guillermo Calleja[†*]

[†]*Department of Chemical, Energy and Mechanical Technology, Rey Juan Carlos University, C/ Tulipán s/n, 28933, Mostoles (Spain).*

[⊥]*Department of Chemical and Environmental Technology, C/ Tulipán s/n, 28933, Mostoles (Spain).*

[§]*Department of Inorganic Chemistry, University of Granada, Avda. Fuentenueva s/n, Granada, (Spain).*

[∇]*Laboratorio de Estudios Cristalográficos, IACT, CSIC-Universidad de Granada, Avda. de las Palmeras 4, 18100 Armilla, Granada, Spain.*

† These authors contributed equally to this work.

*Corresponding Author: guillermo.calleja@urjc.es

1. Synthesis of H_4EBTC

The preparation of the organic linker 5,5-(ethynylene)-diisophthalic acid (**H_4EBTC**) involves five steps. Amine dimethyl 5-aminoisophthalate was used as starting material (Scheme 3). Through its reaction with $NaNO_2$ and KI in toluene, the iodide derivative **1a** was obtained after the purification by recrystallization in MeOH, as a light yellow solid (65 %). Next, the silicon derivative **2a** was obtained through reaction of dimethyl 5-iodoisophthalate **1a** with CuI, PPh_3 and $Pd(PPh_3)_2Cl_2$ in Et_3N as solvent, following by the addition of ethynyltrimethylsilane, with a reaction yield of 80%. This silicon derivative was treated with KF in EtOH as solvent for obtaining the alkine **3a**. Finally, compounds **3a** and **1a** were used in the Sonogashira reaction, which was catalyzed by $Pd(PPh_3)_2Cl_2$ in toluene as solvent. Compound **4a** was purified by column chromatography (SiO_2), with a yield of 67 %, and finally hydrolysed, obtaining the desired ligand **H_4EBTC** with an excellent yield (90 %).

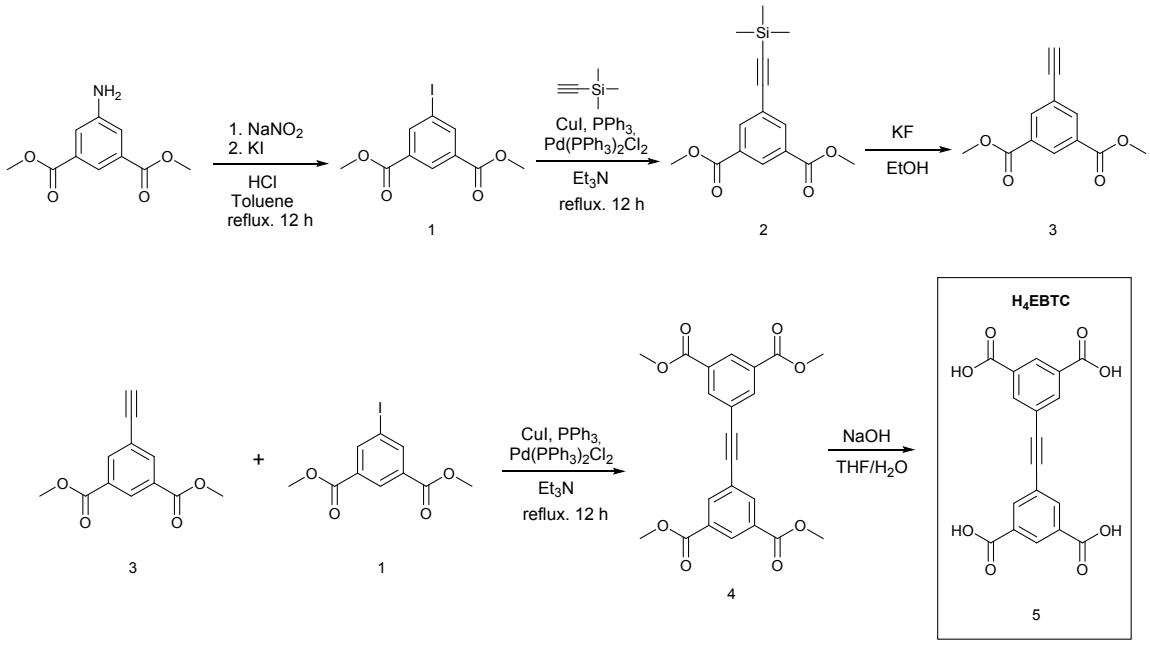

Dimethyl 5-iodoisophthalate (1a):

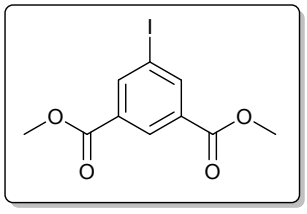

After preparing a suspension of dimethyl 5-aminoisophthalate (5.2 g, 25 mmol) in 6M HCl (15 ml) at 0 ° C, a solution of sodium nitrite 1.7 M (30 mL) was added dropwise under stirring. Next, 40 ml of toluene was added followed by the gradual addition of a solution of 8.2 g of KI previously dissolved in 20 ml of H_2O. The reaction mixture was left under stirring for 12 h. The crude of reaction was then extracted three times with ethyl acetate. The collected organic phases were dried over anhydrous Na_2SO_4 and the solvent was removed under vacuum. The resulting brown oil was recrystallized from methanol, obtaining compound **1** as a light yellow solid (yield: 65%, 5.2 g). ^{1}H RMN (400 MHz, $CDCl_3$): δ = 8.61 (t, J = 1.4 Hz, 1H), 8.53 (d, J = 1.5 Hz, 1H), 3.94 (s, 6H). ^{13}C NMR (101 MHz, $CDCl_3$): δ = 165.00, 142.66, 132.35, 130.06, 93.67, 52.88.

Dimethyl 5-((trimethylsilyl)ethynyl)isophthalate (2a):

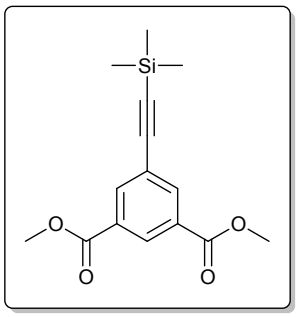

Under nitrogen atmosphere, 2.7 ml of ethinyltrimethylsilane (19 mmol) were added, little by little, to a solution of dimethyl 5-iodoisophthalate **1** (5.2g, 17mmol), CuI (0.6g, 3.1mmol), PPh_3 (0.83g, 3.2mmol) and $Pd(PPh_3)_2Cl_2$ (0.55 g, 0.8 mmol) in anhydrous triethylamine (100 mL). The reaction was left under stirring for 12 h at 90 ° C. After this time, the solvent was evaporated under reduced pressure and the crude obtained was purified by column chromatography (9:1 hexane/AcOEt). Compound **2** was obtained as a pale yellow solid (yield: 80%, 3.9 g). ^{1}H RMN (400 MHz, $CDCl_3$): δ = 8.60 (t, *J* = 1.6 Hz, 1H), 8.29 (d, *J* = 1.6 Hz, 2H), 3.94 (s, 6H), 0.26 (s, 9H). ^{13}C RMN (101 MHz, $CDCl_3$) δ 165.75, 137.06, 131.00, 130.47, 124.40, 102.89, 96.92, 52.74, 0.00.

Dimethyl 5-ethynylisophthalate (3a):

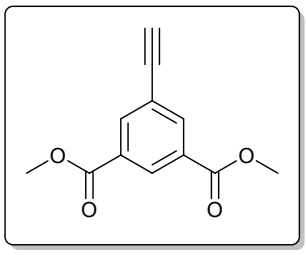

2 g of KF (40.1 mmol) were added a solution of the silicon derivative **2** (3.9 g, 13.6 mmol) in EtOH (50 mL). The reaction mixture was kept under stirring at room temperature for 4 h. Next, the solvent was removed in vacuum. Water was added to dissolve the inorganic salts, and product was extracted three times with ethyl acetate. The organic phase was dried over anhydrous Na_2SO_4 and the solvent was removed in vacuum, obtaining precursor **3** as a light brown solid (yield: 86%, 2.7 g). ^{1}H RMN (400 MHz, $CDCl_3$): δ = 8.64 (t, *J* = 1.6 Hz, 1H), 8.32 (d, *J* = 1.6 Hz, 2H), 3.95 (s, 6H), 3.17 (s, 1H). ^{13}C RMN (101 MHz, $CDCl_3$): δ = 165.65, 137.26, 131.52, 130.88, 123.38, 81.74, 79.42, 52.81.

Tetramethyl 5,5'-(ethyne-1,2-diyl)diisophthalate (4a):

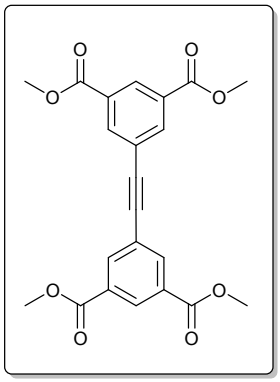

After deoxygenating 200 ml of triethylamine by bubbling a stream of N_2, this solvent was transferred to a round-bottom flask, which contains the iodine derivative **1** (4.3 g, 13.5 mmol), the alkyne **3** (2.7 g, 12.3 mmol), CuI (0.115 g, 0.6 mmol), PPh_3 (0.25 g, 0.95 mmol) and $Pd(PPh_3)_2Cl_2$ (0.24 g, 0.4 mmol). The reaction mixture was heated at 120 ° C for 12 h under stirring and an N_2 atmosphere. After this time, the solvent was removed under reduced pressure and the reaction crude was purified by SiO_2 column chromatography, (8:2 hexane/AcOEt), obtaining compound **4** as a white solid (yield: 67%, 3.37 g). ^{1}H RMN (400 MHz, $CDCl_3$): δ = 8.66 (t, *J* = 1.6 Hz, 1H), 8.38 (d, *J* = 1.6 Hz, 2H), 3.97 (s, 6H). ^{13}C RMN (101 MHz, $CDCl_3$): δ = 160.85, 132.00, 126.50, 125.98, 118.98, 84.52, 48.06.

e) 5,5´-(etine-1,2-diyl)diisophthalic acid (H_4EBTC):

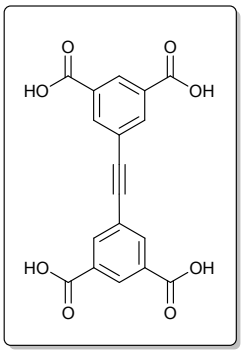

A solution of NaOH (3.286 g, 82 mmol) in 40 ml of H_2O was added to a solution of compound **4** (3.37 g, 8.2 mmol) in 150 ml of THF. The resulting biphasic solution was stirred vigorously at 60 °C for 24 h, before being cooled subsequently to RT. The THF was removed under vacuum to provide typically an insoluble white solid in H_2O. While stirring, the aqueous layer was acidified with concentrated HCl, precipitating a white solid. The resulting precipitate was collected by vacuum filtration and washed with ample water to provide the target compound as typically a white powder. (Yield: 90%, 2.61 g). ^{1}H RMN (400 MHz, DMSO) δ = 8.46 (t, J = 1.6 Hz, 1H), 8.33 (d, J = 1.6 Hz, 2H). ^{13}C RMN (101 MHz, DMSO) δ = 171.21, 141.28, 137.39, 135.57, 128.23, 94.32.

2. ^{1}H and ^{13}C NMR Spectra of H_4EBTC synthesis

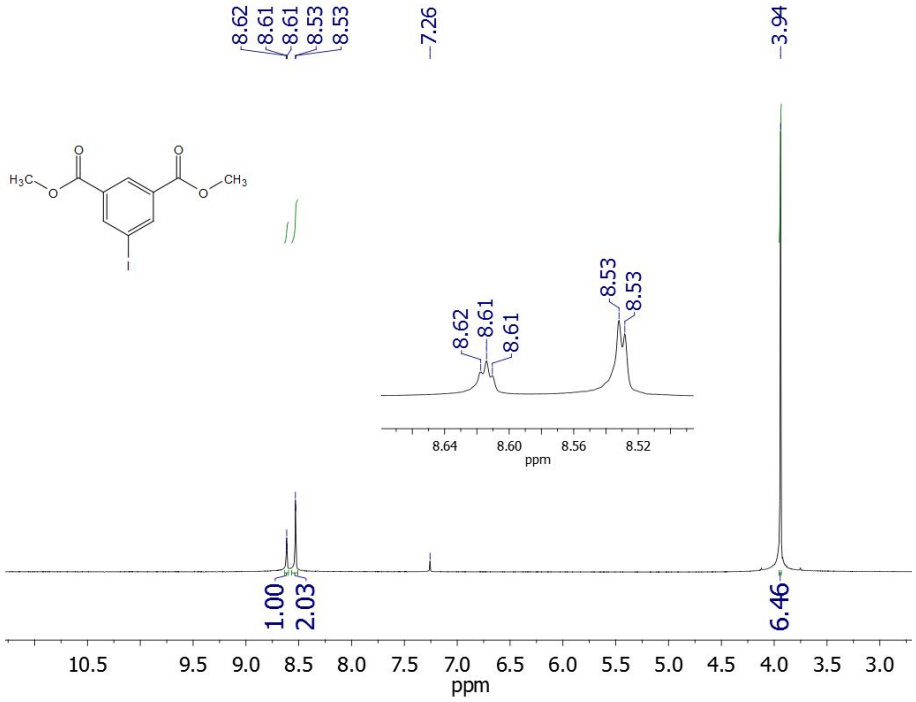

Figure S2.1 ^{1}H-NMR (400MHz, $CDCl_3$, 298K) Compound 1a

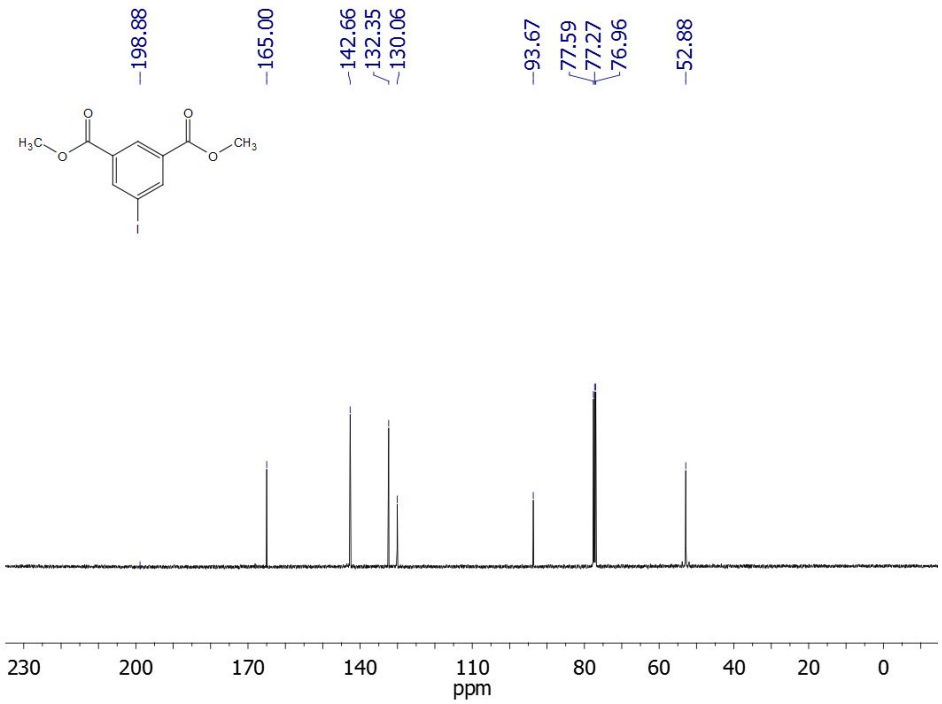

Figure S2. 2 - ^{13}C-NMR (100MHz, $CDCl_3$, 298K) Compound 1a

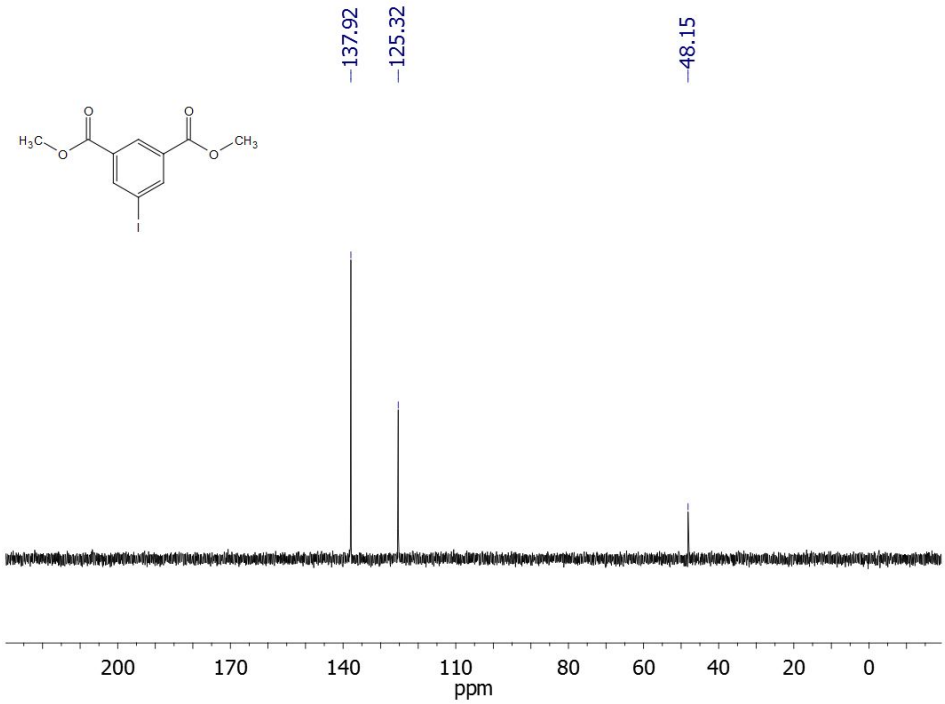

Figure S2 3- ^{13}C-DEPT135 (100MHz, $CDCl_3$, 298K) spectrum of compound 1a

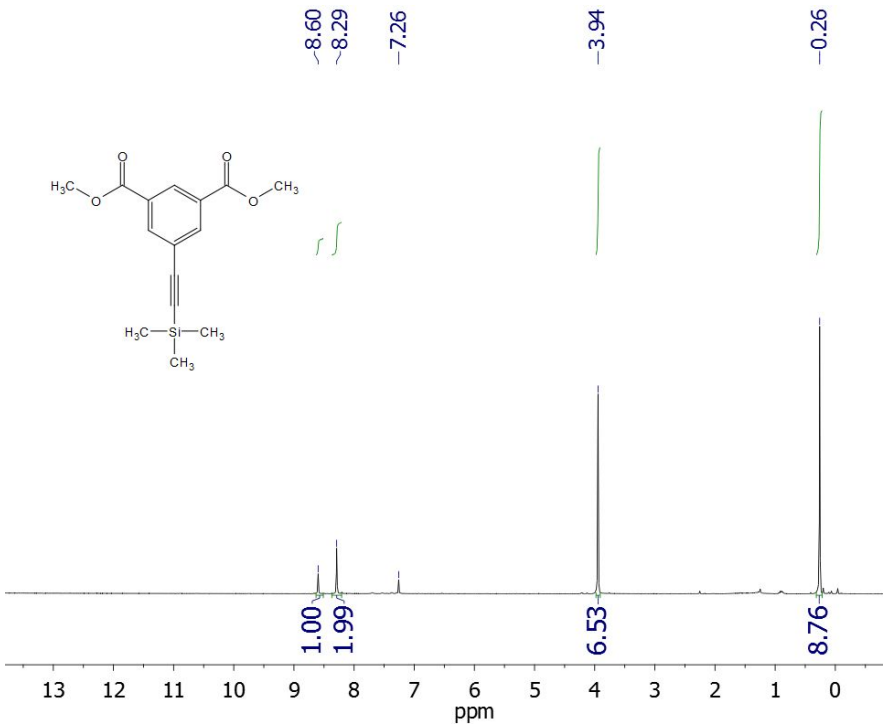

Figure S2.4 ^{1}H-NMR (400MHz, $CDCl_3$, 298K) Compound 2a

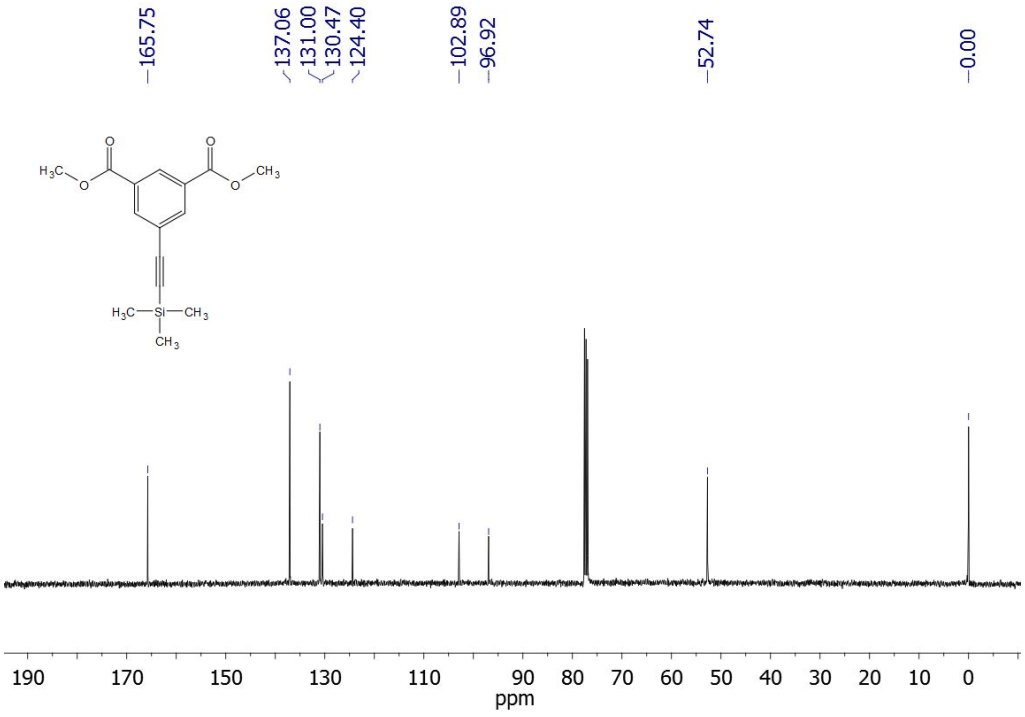

Figure S2. 5 - ^{13}C-NMR (100MHz, $CDCl_3$, 298K) Compound 2a

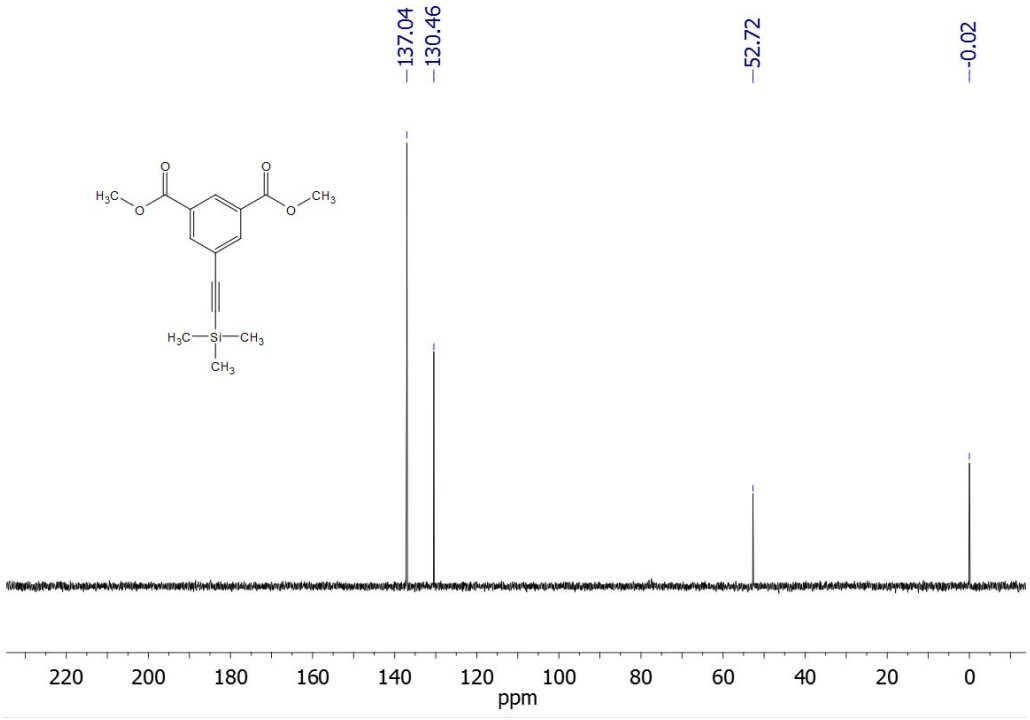

Figure S2. 6- ^{13}C-DEPT135 (100MHz, $CDCl_3$, 298K) spectrum of compound 2a

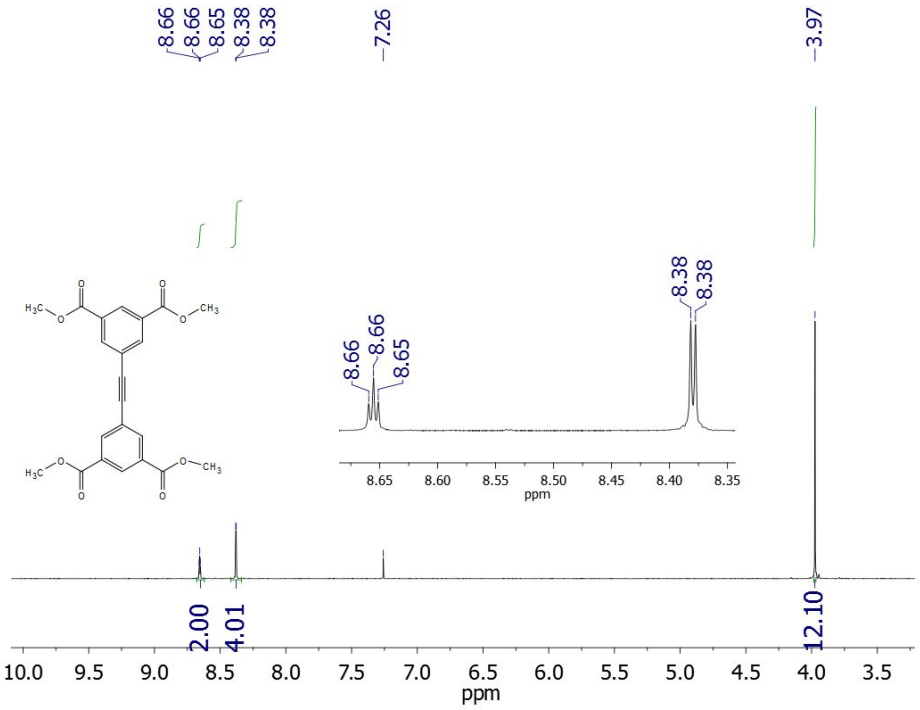

Figure S2.7 ^{1}H-NMR (400MHz, $CDCl_3$, 298K) Compound 3a

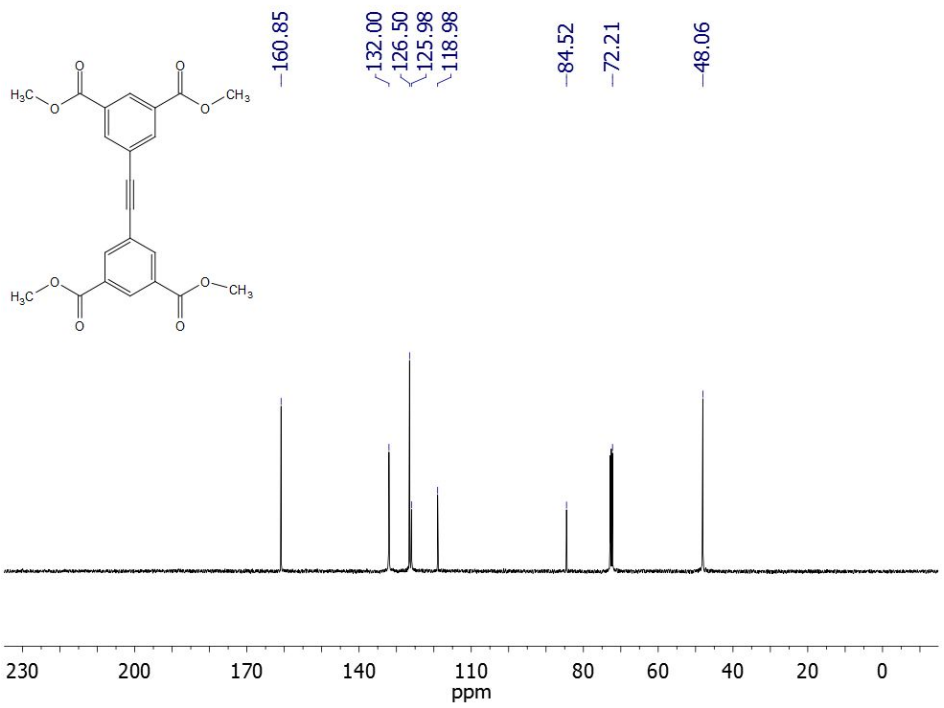

Figure S2. 8 - ^{13}C-NMR (100MHz, $CDCl_3$, 298K) Compound 3a

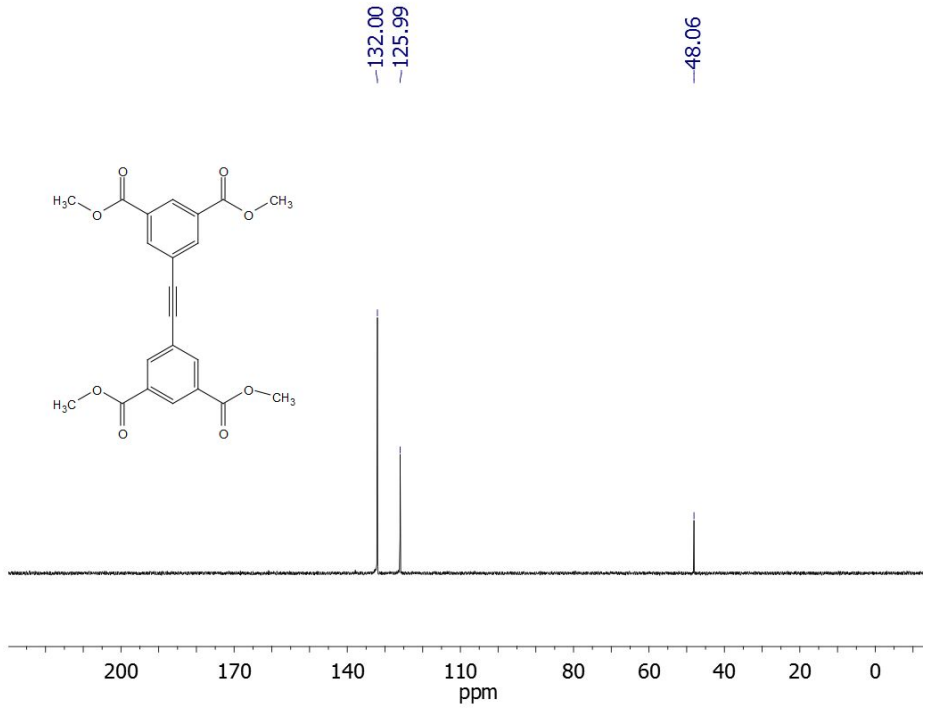

Figure S2. 9- ^{13}C-DEPT135 (100MHz, $CDCl_3$, 298K) spectrum of compound 3a

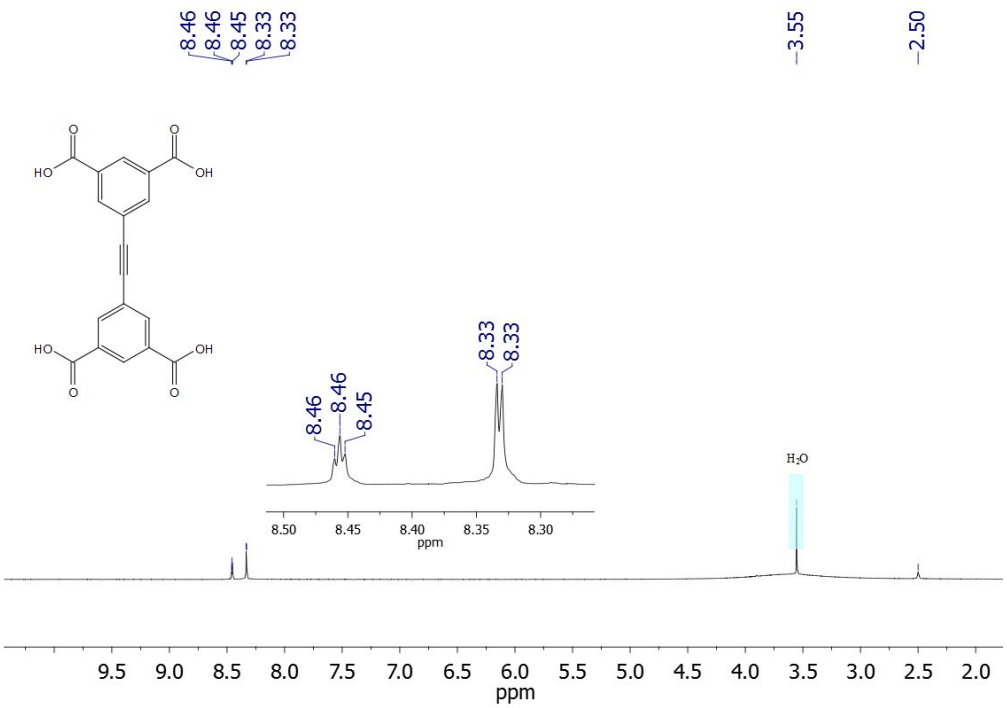

Figure S2.10 ^{1}H-NMR (400MHz, DMSO-d^{6}, 298K) Compound H_4EBTC

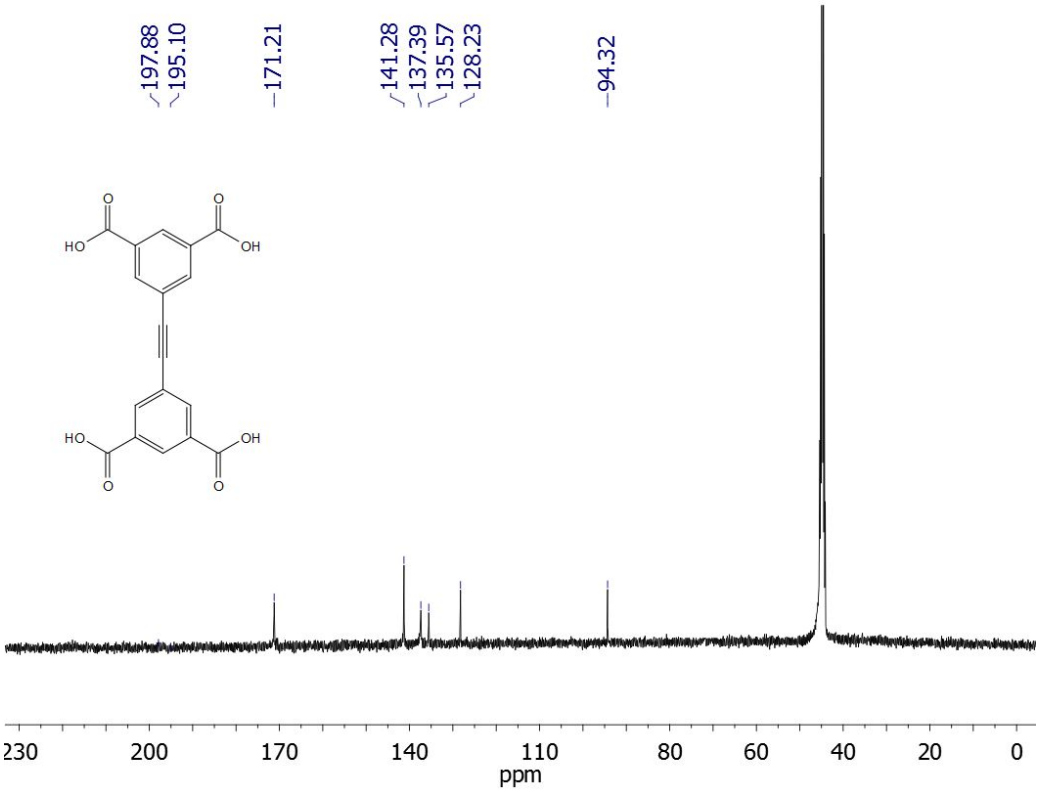

Figure S2. 11 - ^{13}C-NMR (100MHz, DMSO-d^{6}, 298K) Compound H_4EBTC

3. Crystallographic data of Co-URJC-4

The data processing was performed with the APEX3[1] software and corrected for absorption using SADABS.[2] Crystal structure was solved by intrinsic phasing method using the SHELXT program and refined by full-matrix least-squares on F^2 including all reflections using anisotropic displacement parameters.[3] The OLEX2 software was used as a graphical interface.[4] All hydrogen atoms were included as fixed contributions riding on attached atoms with isotropic thermal displacement parameters 1.2 times or 1.5 times those of their parent atoms for the organic ligands. The crystal is a two-component nonmerohedral twin (0.49:0.51). The TWINROTMAT routine in PLATON was used to The TWINROTMAT routine in PLATON[5] was used to find the twin law that describes a rotation of 180º around the [0 0 1] direction, given by the matrix (-1 0 0 0 -1 0 0 0 1). Even though crystal data was collected up to 0.81 Å resolution, crystals still diffracted quite weakly at high angle due to their rather low quality and data were cut off according to intensity statistics, using restraints and constraints during refinement. During refinement, a number of ISOR and RIGU restraints had to be used to obtain reasonable displacement parameters for all non-hydrogen atoms. Their Uij values were therefore restrained to be approximately spherical. Severely disordered DMF molecules could not be modeled reasonably and were therefore removed from the diffraction data (using the SQUEEZE routine in PLATON) but considered for calculation of empirical formula, formula weight, density, linear absorption coefficient and F(000).

Table S3.1. Crystal data and structure refinement for Co-URJC-4

Parameter	Value	
Empirical formula	$C_{270}H_{354}Co_{16}N_{42}O_{113}$	
Formula weight	6938.81	
Temperature	100(2) K	
Wavelength	1.54178 Å	
Crystal system	Monoclinic	
Space group	$P2_1/c$	
Unit cell dimensions	a = 19.1972(8) Å b = 38.1664(17) Å c = 47.308(2) Å	α= 90°. β= 90.105(2)°. y = 90°.
Volume	34662(3) $Å^3$	
Z	4	
Density (calculated)	1.330 Mg/m^3	
Absorption coefficient	6.561 mm^{-1}	
F(000)	14416	
Crystal size	0.12 x 0.12 x 0.08 mm^3	
Theta range for data collection	2.197 to 39.971°.	
Index ranges	-15<=h<=15, -31<=k<=31, 0<=l<=39	

Reflections collected	20419
Independent reflections	20419 [R(int) = 0.0217]
Completeness to theta = 39.971°	97.3 %
Absorption correction	Semi-empirical from equivalents
Max. and min. transmission	0.7490 and 0.4942
Refinement method	Full-matrix least-squares on F^2
Data / restraints / parameters	20419 / 3874 / 2635
Goodness-of-fit on F^2	1.055
Final R indices [I>2sigma(I)]	R1 = 0.1367, wR2 = 0.3439
R indices (all data)	R1 = 0.1460, wR2 = 0.3527
Extinction coefficient	n/a
Largest diff. peak and hole	1.570 and -1.029 e.$Å^{-3}$

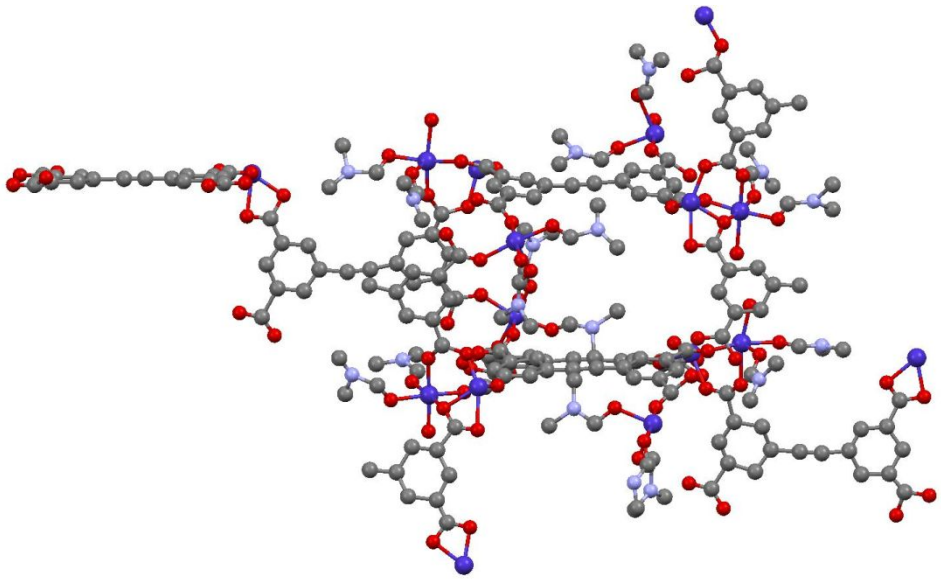

Figure S3.1 Asymmetric unit of Co-URJC-4 material. Dark blue = cobalt; grey = carbon; red = oxygen; light blue = nitrogen. Hydrogen atoms are omitted for clarity

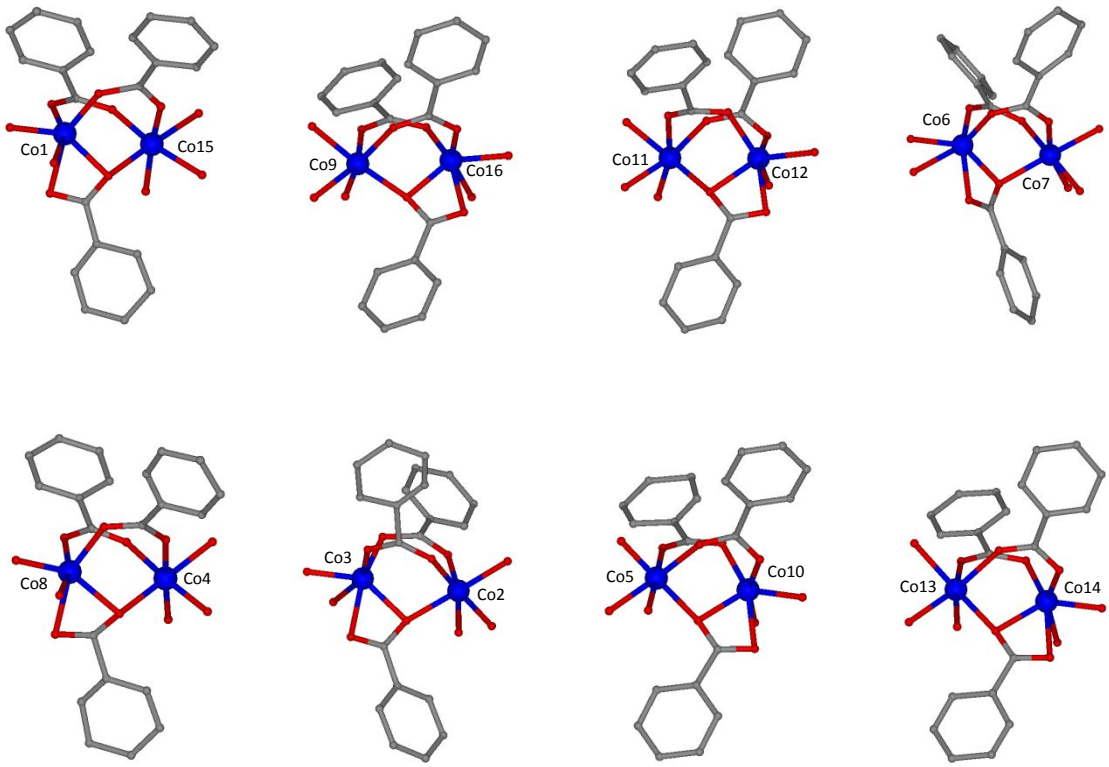

Figure S3.2 Eight different cobalt dimeric cluster presents in the asymmetric unit of Co-URJC-4.

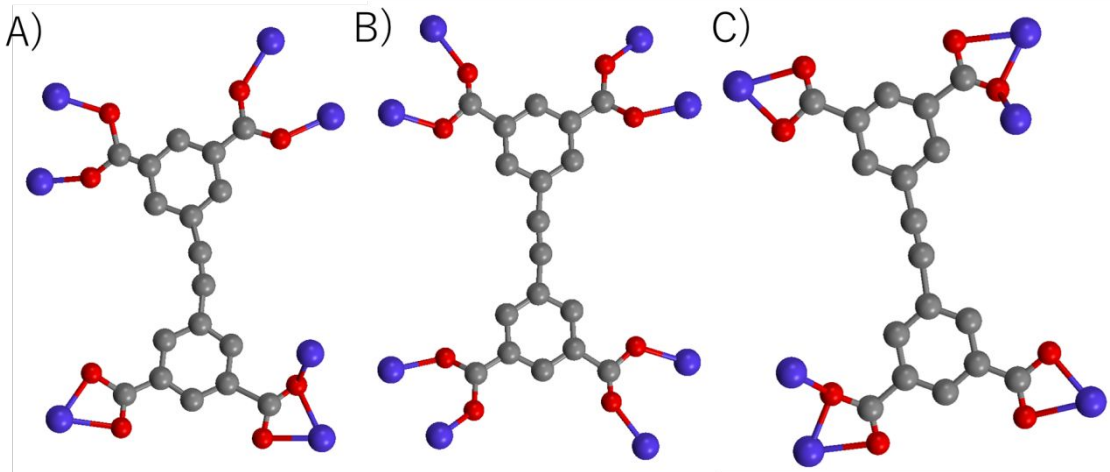

Figure S3.3. Coordination mode of H4EBTC ligand in Co-URJC-4 material. Purple = cobalt; grey = carbon; red = oxygen; light blue = nitrogen. Hydrogen atoms are omitted for clarity

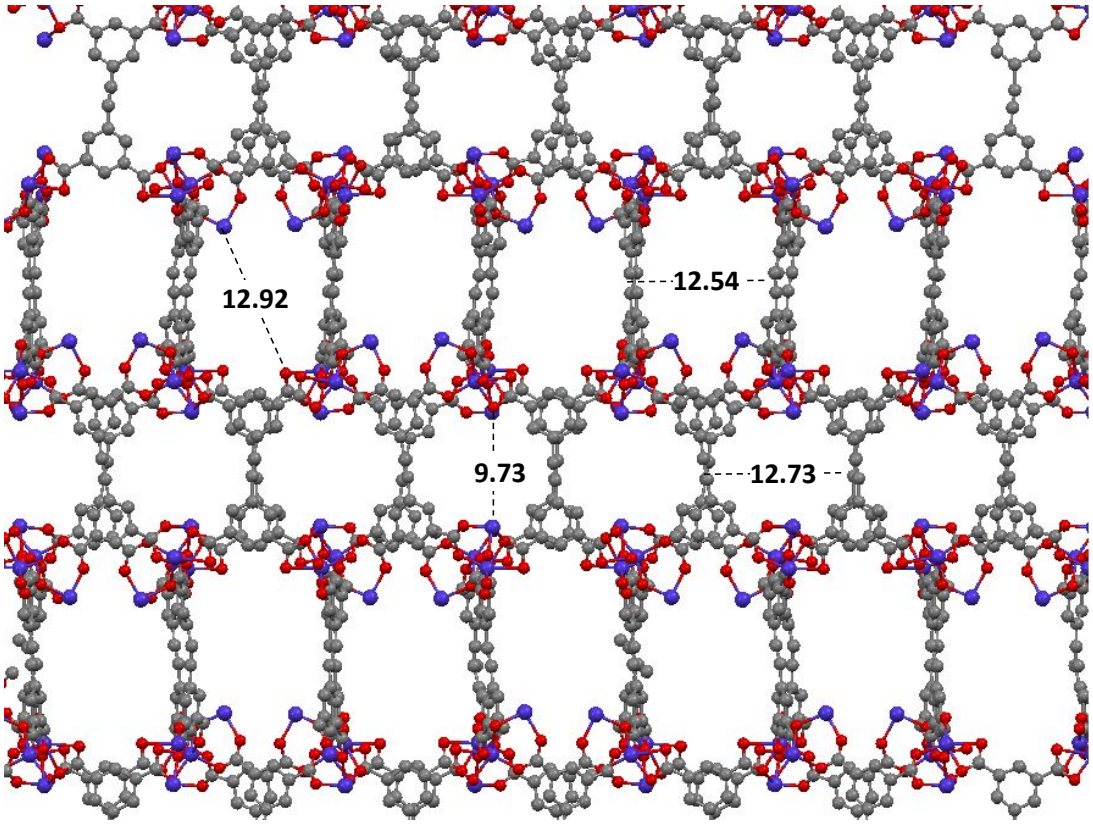

Figure S3.4. Co-URJC4 guest free packing along a axis. Purple = cobalt; grey = carbon; red = oxygen; light blue = nitrogen. Hydrogen atoms are omitted for clarity

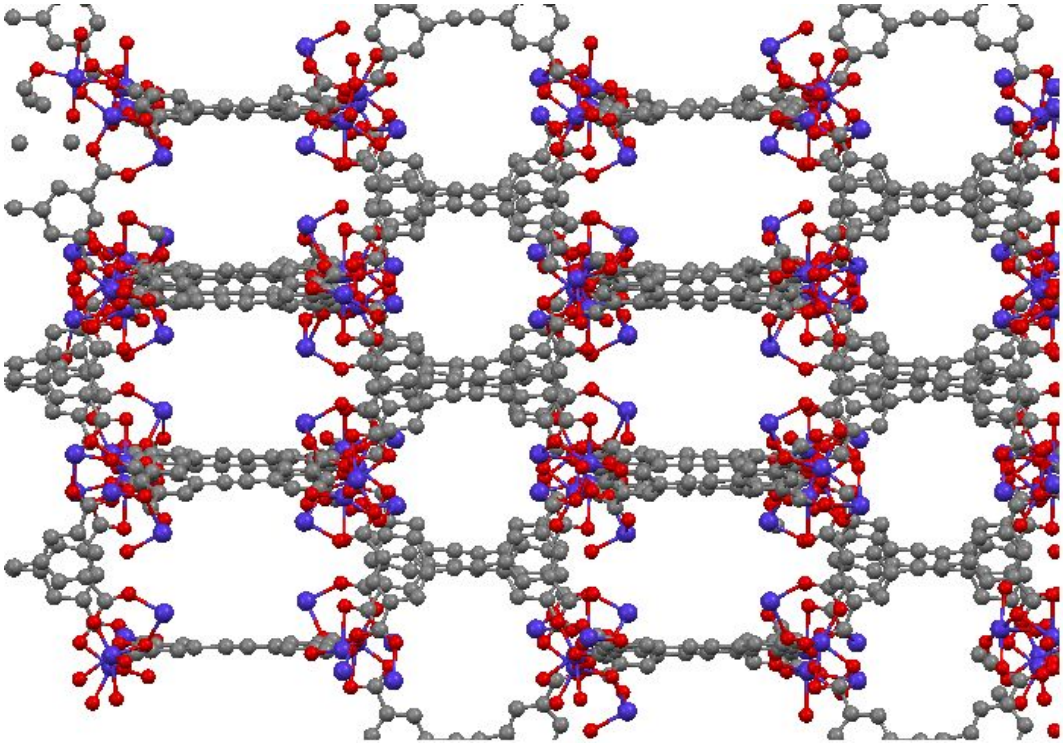

Figure S3.5. Co-URJC4 guest free packing along b axis. Purple = cobalt; grey = carbon; red = oxygen; light blue = nitrogen. Hydrogen atoms were omitted for clarity

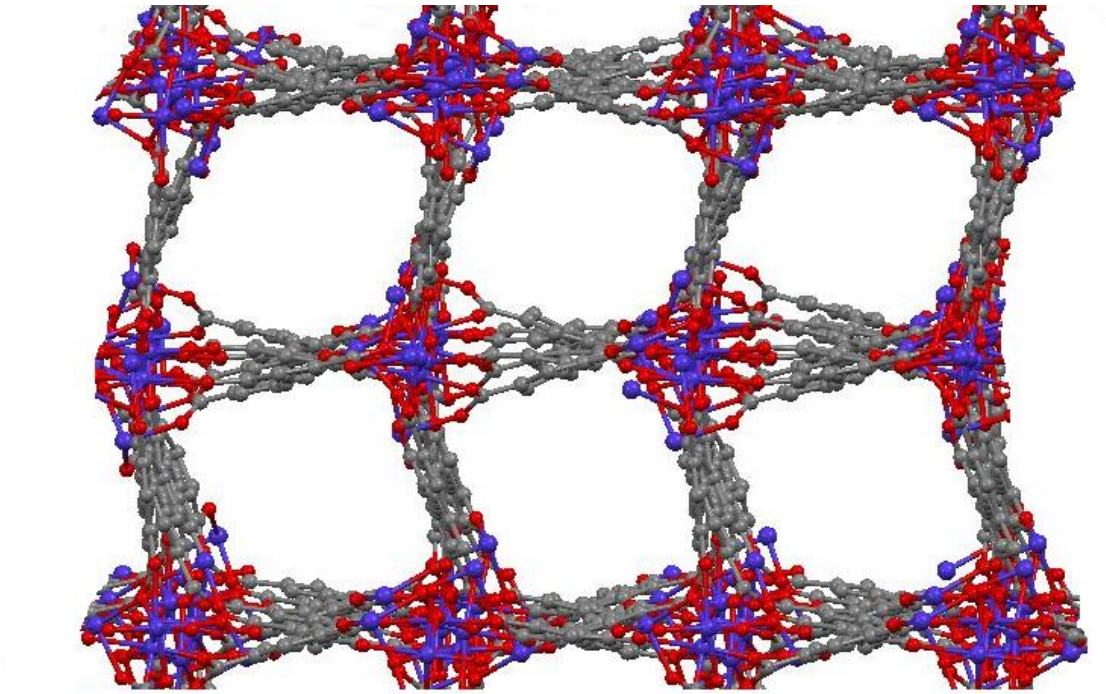

Figure S3.6. Co-URJC4 guest free packing along c axis. Purple = cobalt; grey = carbon; red = oxygen; light blue = nitrogen. Hydrogen atoms were omitted for clarity

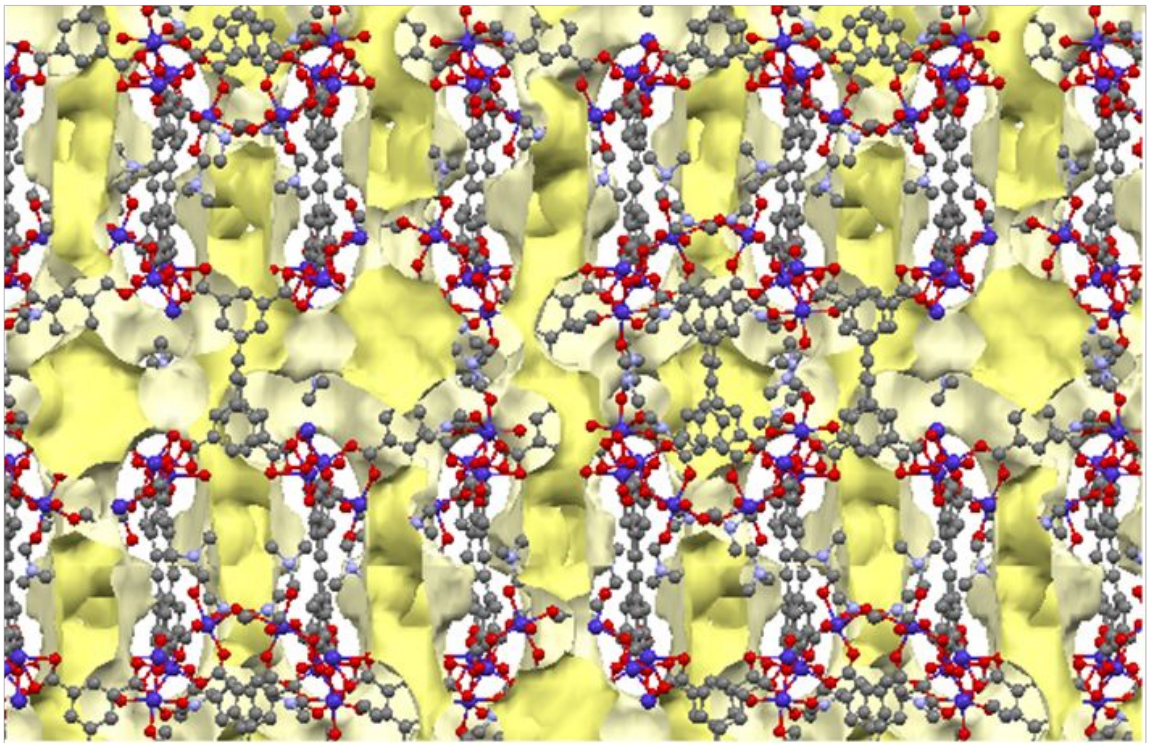

Figure S3.7. Void channel system of Co-URJC4 material along a axis. Dark blue = cobalt; grey = carbon; red = oxygen; light blue = nitrogen. Hydrogen atoms were omitted for clarity

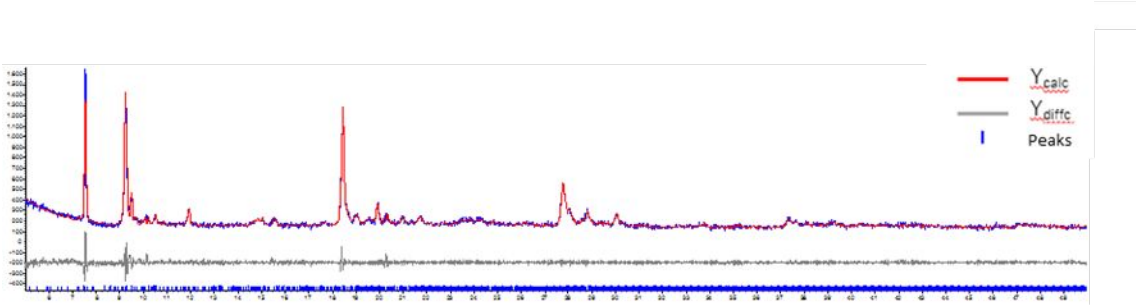

Figure S3.8. Le Bail fitting of Co-URJC-4

Table S3.2. Crystallographic data of Co-URJC-4

Space group	a [Å]	b [Å]	c [Å]	α [º]	β [º]	γ [º]	V [Å³]
$P2_1/c$	19.18	38.08	47.36	90	90	90	34596.48

4. XRD refinement of Ni-URJC-4

Co-URJC-4 was used as starting model, where the Co ions were replaced by Ni, and only the coordinates of the Ni ions were refined. In addition, the lattice parameters, thermal parameters for Ni, and 10 Chebychev-type background parameters, sample displacement, and crystallite size (using a Double-Voight approach with fundamental peak (FP) parameters) were refined using the program TOPAS (version 5, Bruker AXS, Germany). There is good agreement between the data and the model.

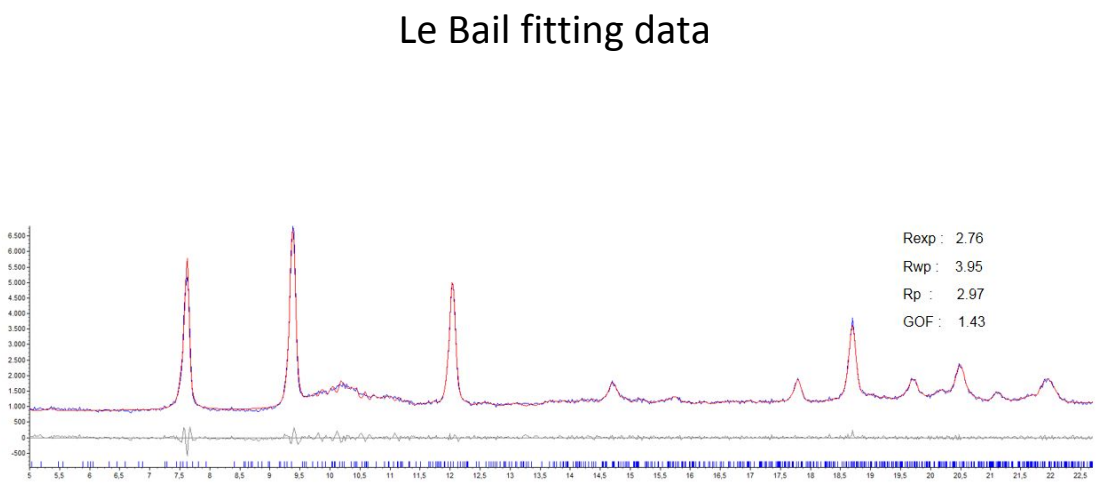

Figure S4.1. Le Bail fitting of Ni-URJC-4

Global R-Values

Rexp: 2.76	Rwp: 3.95	Rp: 2.97	GOF: 1.43
Rexp`: 8.84	Rwp`: 12.66	Rp`: 13.29	DW: 1.28

Instrument

Simple axial model (mm) 6.333(99)

Corrections

Specimen displacement 0.3091(23)

R-Bragg: 0.416
Cry size Lorentzian (nm): 189.5(49)

Table S4. Crystallographic data of Ni-URJC-4

Space group	a [Å]	b [Å]	c [Å]	α [º]	β [º]	γ [º]	V [Å^3]
$P2_1/c$	19.0947(24)	37.9122(49)	47.5186(64)	90	91.294(14)	90	34391.0(78)

5. Characterization of Co-URJC-4 and Ni-URJC-4

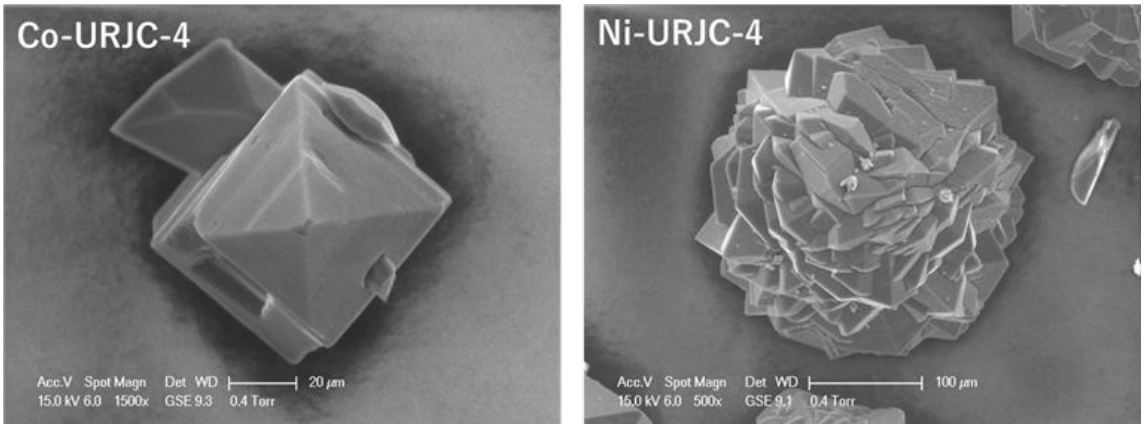

Figure S5.1 SEM micrographs of the as-synthesized URJC-4 samples

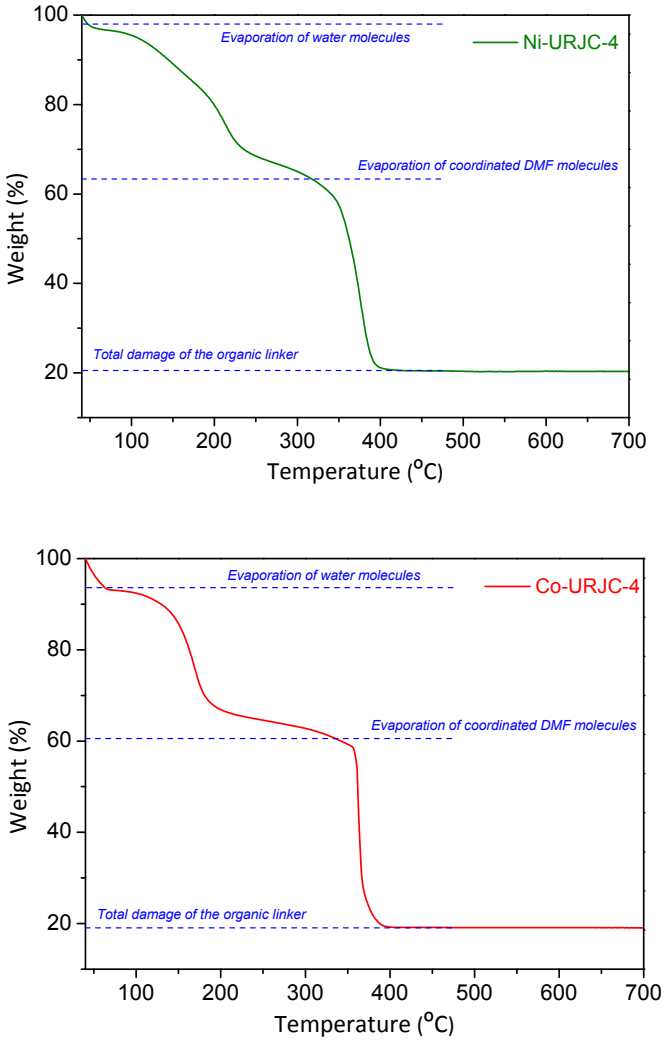

Figure S5.2 TGA analyses of URJC-4 samples.

Table S5. Weight losses from TGA for URJC-4 materials

Ni-URJC-4

	Theoretical (%)	*Experimental (%)*
H_2O	2	1
DMF	42	38
Organic ligand	41	41
Ni	15	20

Co-URJC-4

	Theoretical (%)	*Experimental (%)*
H_2O	2	6
DMF	42	39
Organic ligand	41	38
Co	15	17

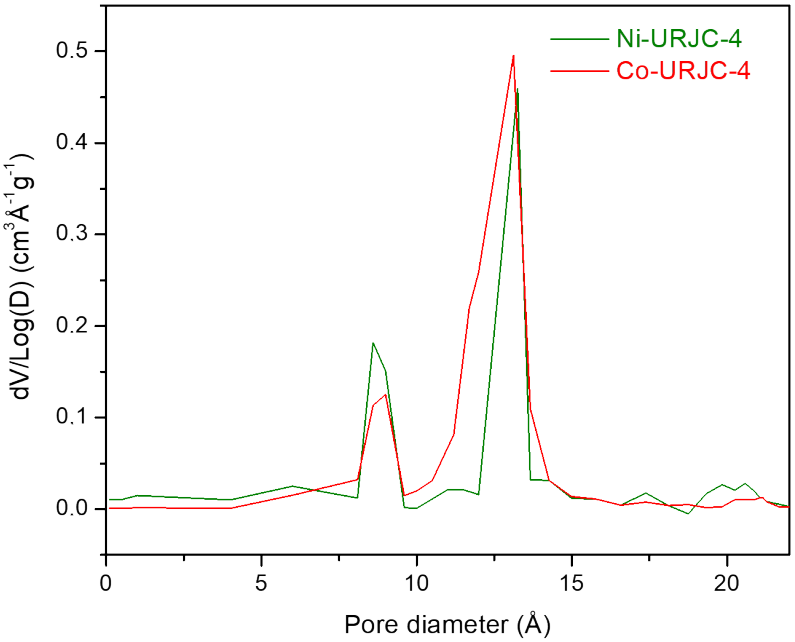

Figure S5.3 Pore size distribution of URJC-4 samples

Ni-URJC-4 material was experimentally compared with the well-known Ni-MOF-74, among the best ones for H_2 retention. Figures below for the two Ni MOF materials show the H_2 adsorption isotherms at 298 K and high pressure in both units: total volumetric and excess gravimetric, where it is observed that Ni-URJC-4 surpasses Ni-MOF-74 for all cases at high pressure.

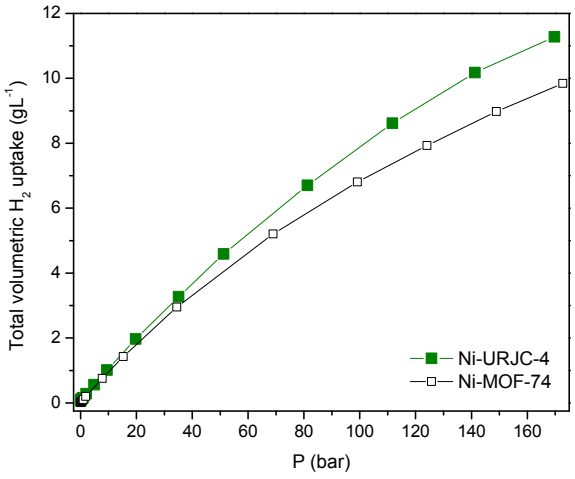

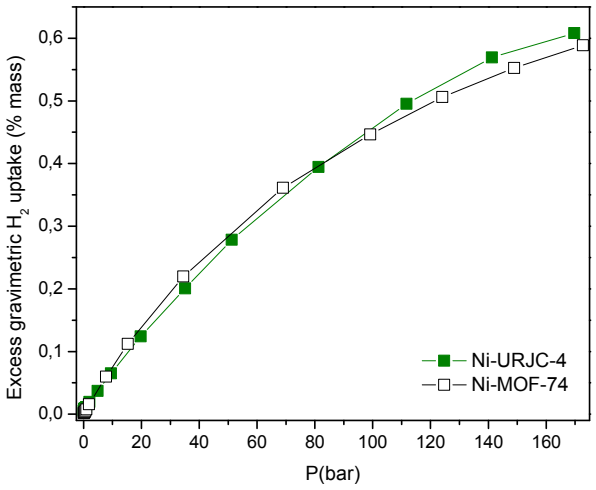

Figure S5.4 H_2 adsorption isotherms at 298K for Ni-URJC-4 and Ni-MOF-74 materials.

Moreover, we completed the analysis by comparing the relative H_2 adsorption capacity per m^2, normalizing the hydrogen adsorbed in excess, i.e. dividing by the BET surface area of each material. As a result, it is evidenced the higher amount of H_2 adsorbed per m^2 (higher affinity) of Ni-URJC-4:

Ni-URJC-4: 0.6/829 = 7.24 e-4 %mass/m^2
Ni-MOF-74: 0.58/1325 = 4,44 e-4 %mass/m^2

In addition, we also estimated the adsorbed H_2/nickel at room temperature for both materials, from the amount of adsorbed H_2 in excess and the molar weight of the MOF structure. It can be observed that again Ni-URJC-4 has a higher adsorption capacity per metal than Ni-MOF-74.

Ni-URJC-4: 0.59 mol H_2/mol Ni
Ni-MOF-74: 0.38 mol H_2/mol Ni

6. Chemical stability of URJC-4 materials

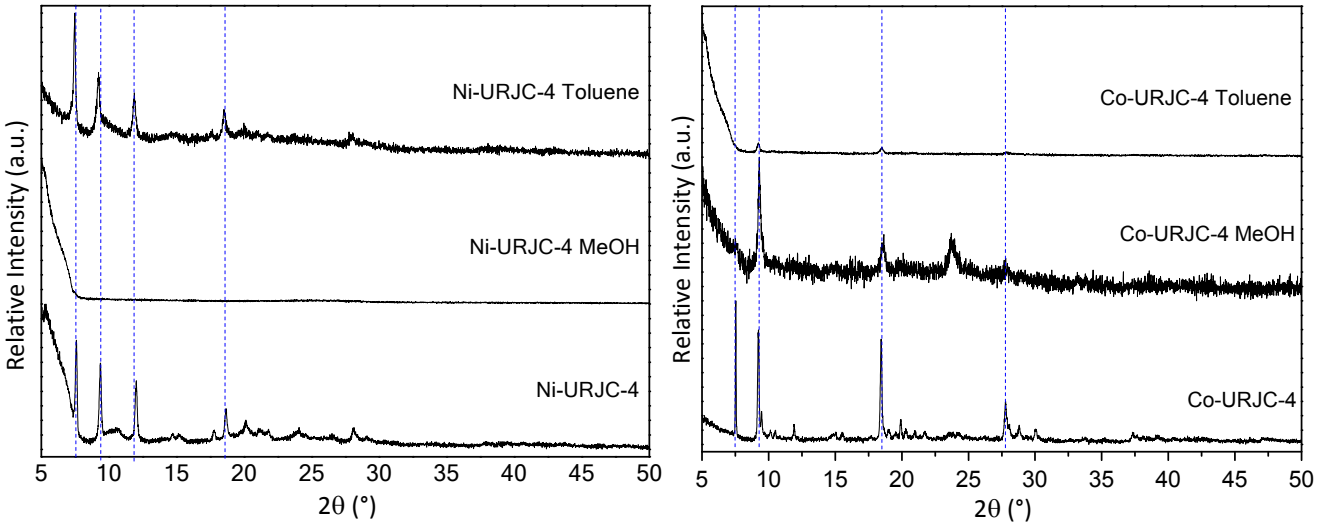

Figure S6. XRD patterns of the URJC-4 materials after suspension in methanol and toluene.

7. Catalytic tests installation

After activating the MOF at 150 °C for 12 h under vacuum, 15 mg of this catalyst, 60 mg of the carbonyl compound and 1.4 eq of the corresponding primary amine were mixed in toluene (15 mL) and put into a 50 mL stainless steel high-pressure reactor (Figure S7). The temperature of the reactor was increased and maintained at 115 ° C, and the reactor was pressurized with H_2 (99.999%) up to 5.0 bar. The reaction vessel was kept connected to a H_2 source throughout the reaction via a one-way check valve to maintain the pressure at the desired level. The reaction mixture was stirred (200 rpm) under the pressurized conditions for a period of 18 h. When the reaction was completed, the reactor was quickly cooled down in cold water, and then pressure was released slowly.

Figure S7. Reactor running a catalytic test on Reactor BüchiGlasUster™ with a sand bath.

8. ^{1}H and ^{13}C NMR Spectra of amine products

Compound 1: N-benzylbutanamine[6]

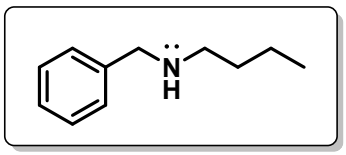

Yield: 76% (Colorless Oil)

^{1}H-NMR (400 MHz, $CDCl_3$) δ: 7.42-7.29 (5H, m), 4.41 (1H, s), 3.90 (2H, m), 2.70 (2H, t, *J= 6.1 Hz*), 1.65-1.49 (2H, m), 1.46-1.35 (2H, m), 0.97 (3H, t, *J=5.9 Hz*)

^{13}C-NMR (100 MHz, $CDCl_3$) δ: 133.6, 129.9, 129.1, 128.7, 128.7, 128.2, 127.6, 52.1, 47.4, 29.3, 20.0, 13.4. MS(ESI): m/z calcd. for $C_{11}H_{17}N$: 163.14, found $[M+H]^+$: 164.11

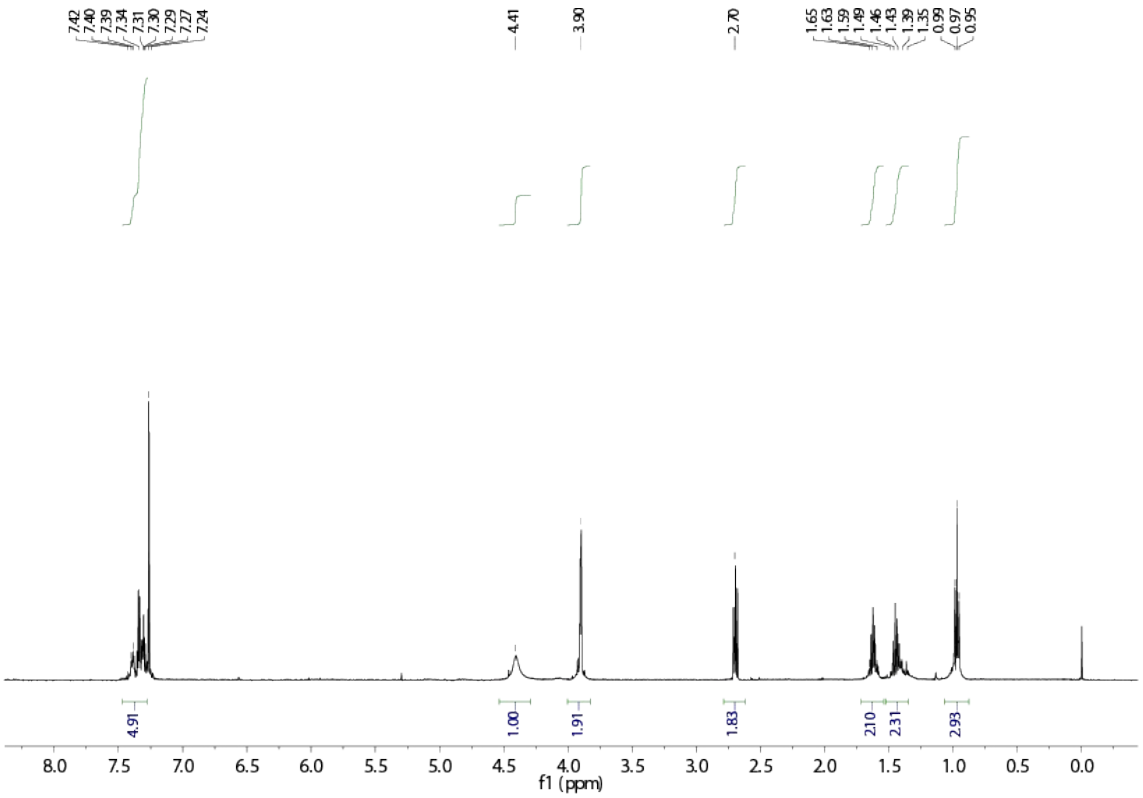

Figure S8.1 ^{1}H-NMR (400MHz, $CDCl_3$, 298K) Compound 1

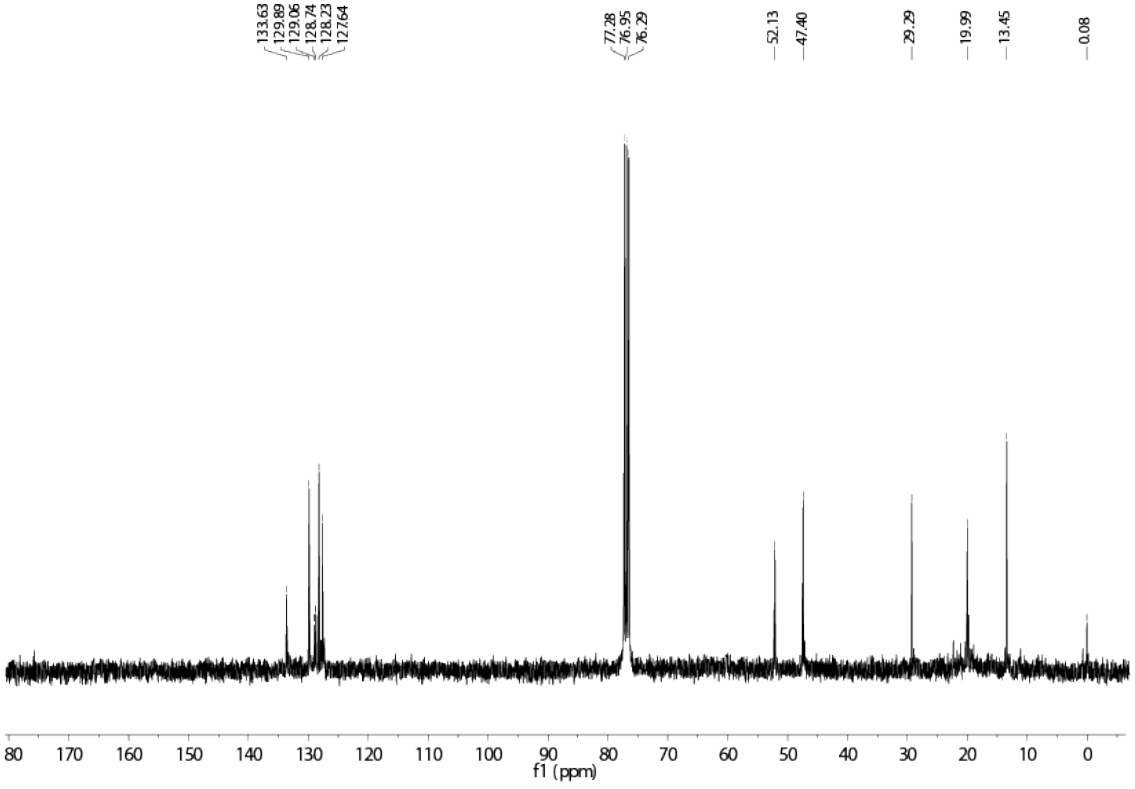

Figure S8. 2 - ^{13}C-NMR (100MHz, $CDCl_3$, 298K) Compound 1

Compound 2: N-(Diphenylmethyl)butanamine[7]

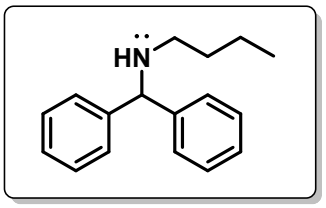

Yield: 86% (Pale Yellow Oil)

^{1}H-NMR (400 MHz, $CDCl_3$) δ: 7.45-7.39 (4H, m), 7.32-7.30 (2H, m), 7.28-7.16 (4H, m), 4.84 (1H, s), 2.65-2.60 (2H, m), 1.68 (1H, bs), 1.58-1.53 (2H, m), 1.43-1.37 (2H, m), 0.91 (3H, t, *J=7.6 Hz*)

^{13}C-NMR (100 MHz, $CDCl_3$) δ: 144.2, 128.4, 127.9, 127.5, 126.7, 126.1, 67.6, 48.1, 32.4, 20.4, 14.0

MS(ESI): m/z calcd. for $C_{17}H_{21}N$: 239.17, found : 239.25

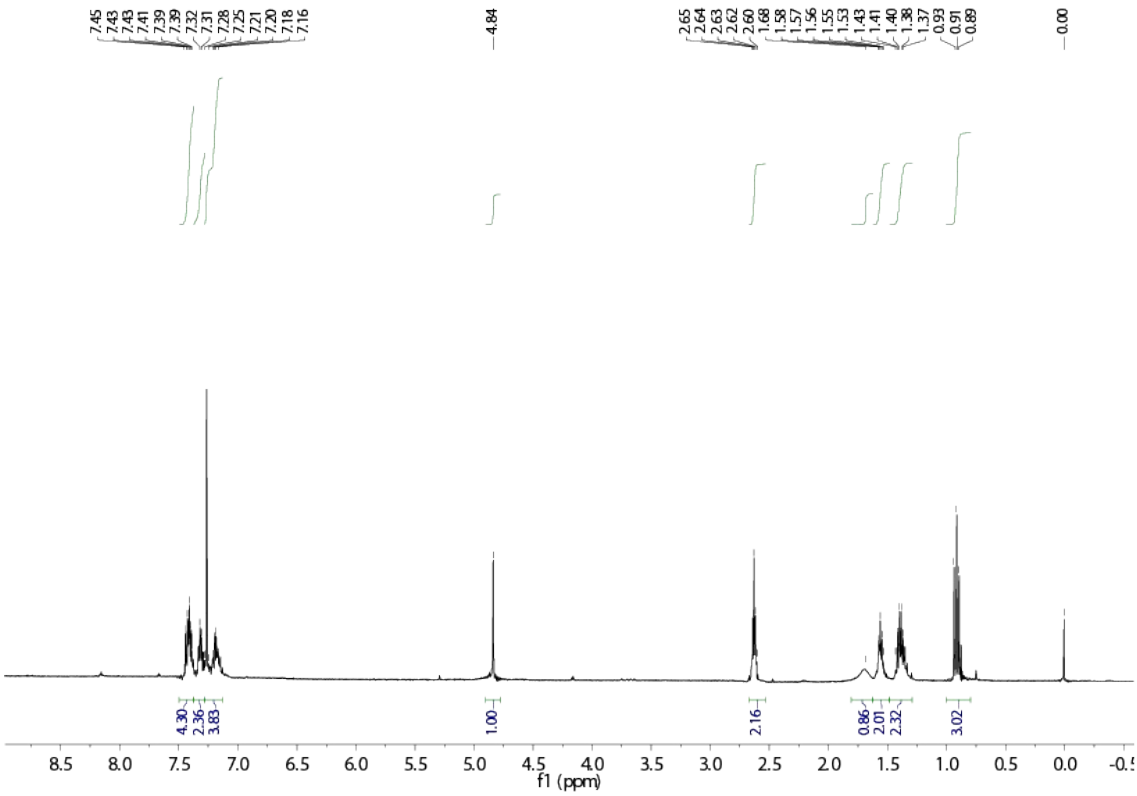

Figure S8.3 ^{1}H-NMR (400MHz, $CDCl_3$, 298K) Compound 2

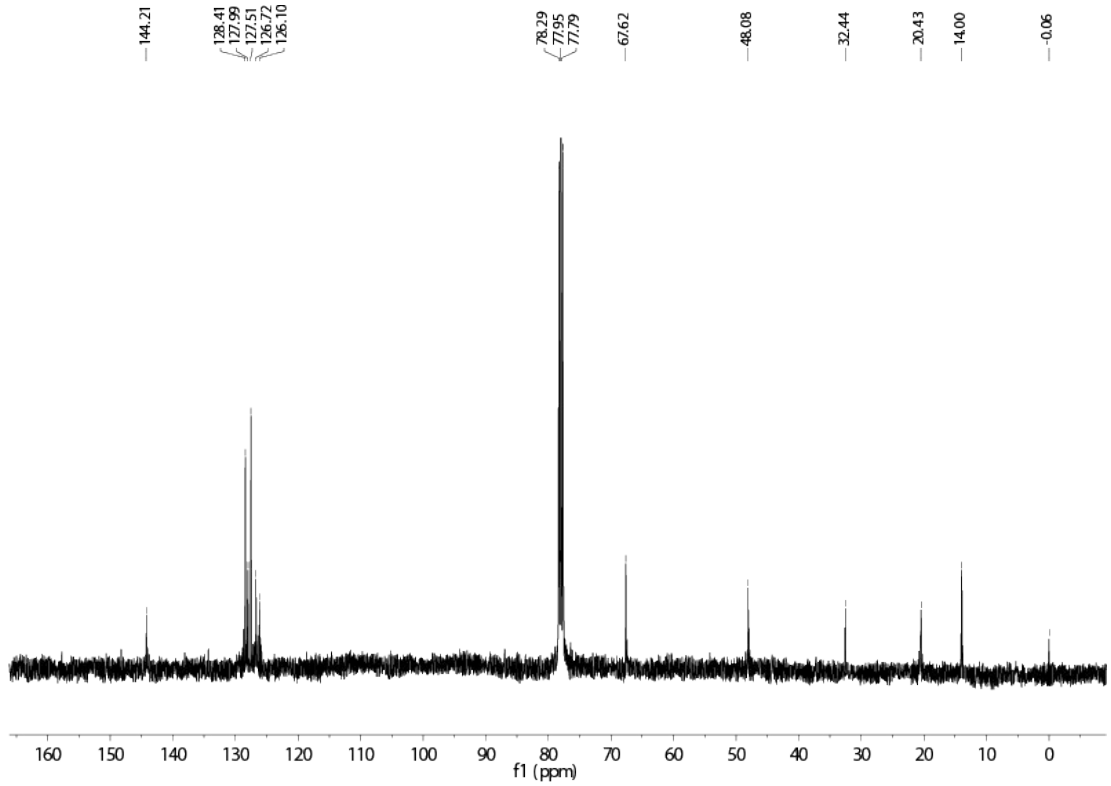

Figure S8. 4 - ^{13}C-NMR (100MHz, $CDCl_3$, 298K) Compound 2

Compound 3: N-benzylaniline[8]

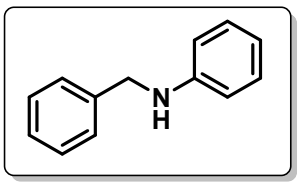

Yield: 79% (Pale Yellow Oil)

^{1}H-NMR (400 MHz, $CDCl_3$) δ: 7.52-7.40 (4H, m), 7.38-7.34 (1H, m), 7.32-7.27 (2H, m), 6.84 (1H, m), 6.70 (2H, t, *J=7.5 Hz*), 4.42 (2H, s), 4.08 (1H, bs)

^{13}C-NMR (100 MHz, $CDCl_3$) δ: 148.3, 139.6, 128.9, 128.9, 128.9, 128.7, 127.6, 127.2, 126.8, 126.3, 112.9, 111.9, 48.5

MS(ESI): m/z calcd. for $C_{13}H_{13}N$: 183.26, found $[M+H]^+$: 184.11

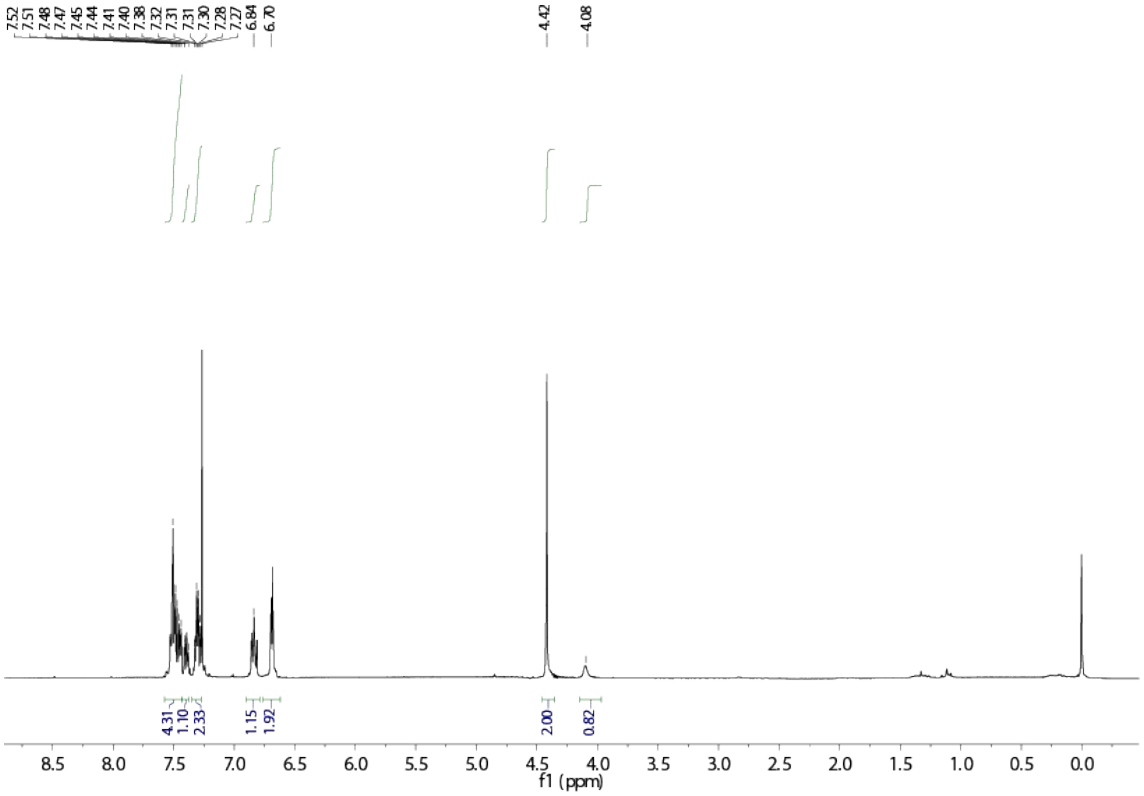

Figure S8.5 ^{1}H-NMR (400MHz, $CDCl_3$, 298K) Compound 3

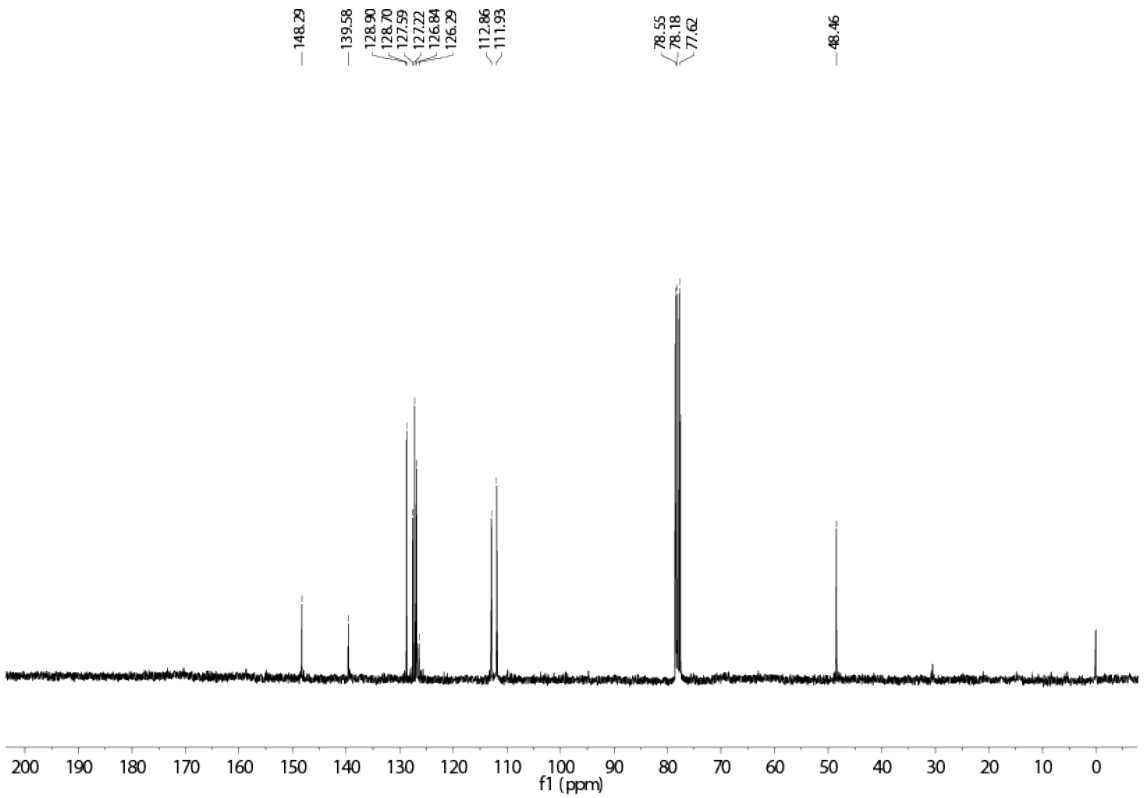

Figure S8. 6 - ^{13}C-NMR (100MHz, $CDCl_3$, 298K) Compound 3

Compound 4: N-benzhydrylaniline[9]

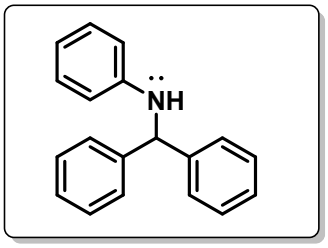

Yield: 83% (Pale Yellow Oil)

^{1}H-NMR (400 MHz, $CDCl_3$) δ: 7.47-7.34 (10H, m), 7.20-7.17 (2H, m), 6.78-6.74 (1H, m), 6.61 (2H, d, J= 7.1 Hz), 5.58 (1H, s), 4.28 (1H, bs)

^{13}C-NMR (100 MHz, $CDCl_3$) δ: 147.4, 142.8, 129.2, 128.4, 127.7, 126.6, 126.4, 62.9

MS(ESI): m/z calcd. for $C_{19}H_{17}N$: 259.14, found: 259.11

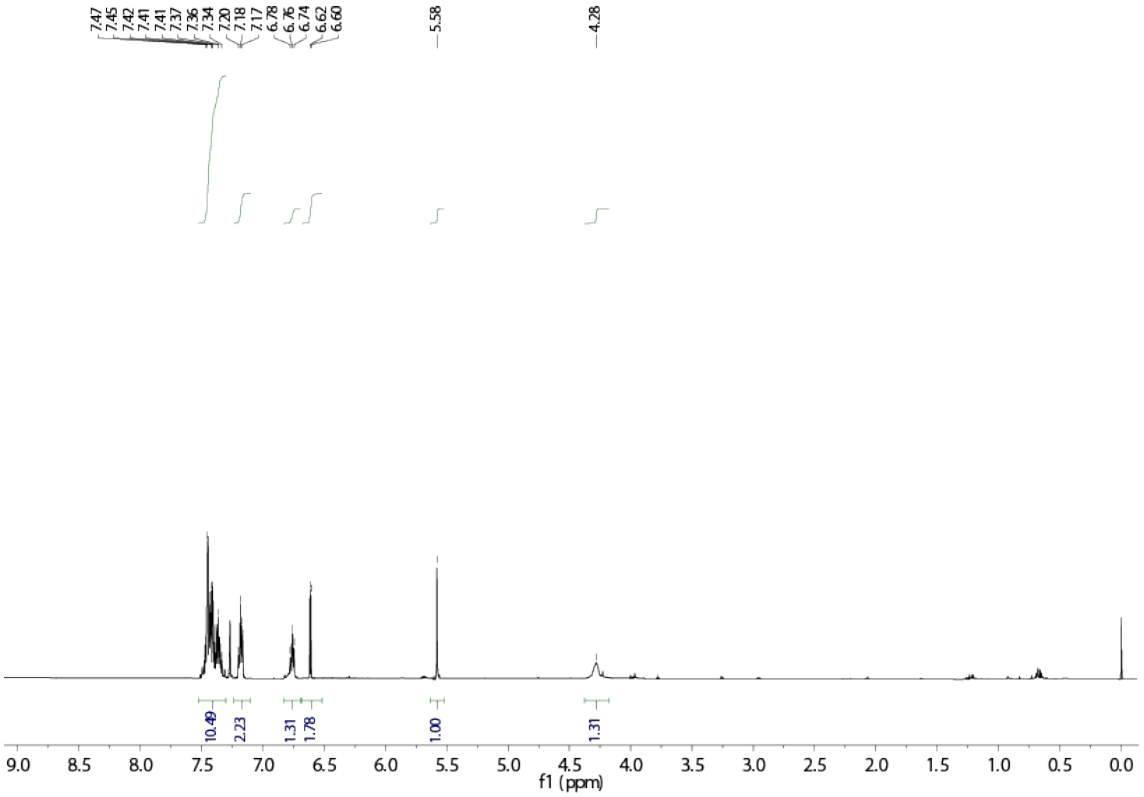

Figure S8.7 ^{1}H-NMR (400MHz, $CDCl_3$, 298K) Compound 4

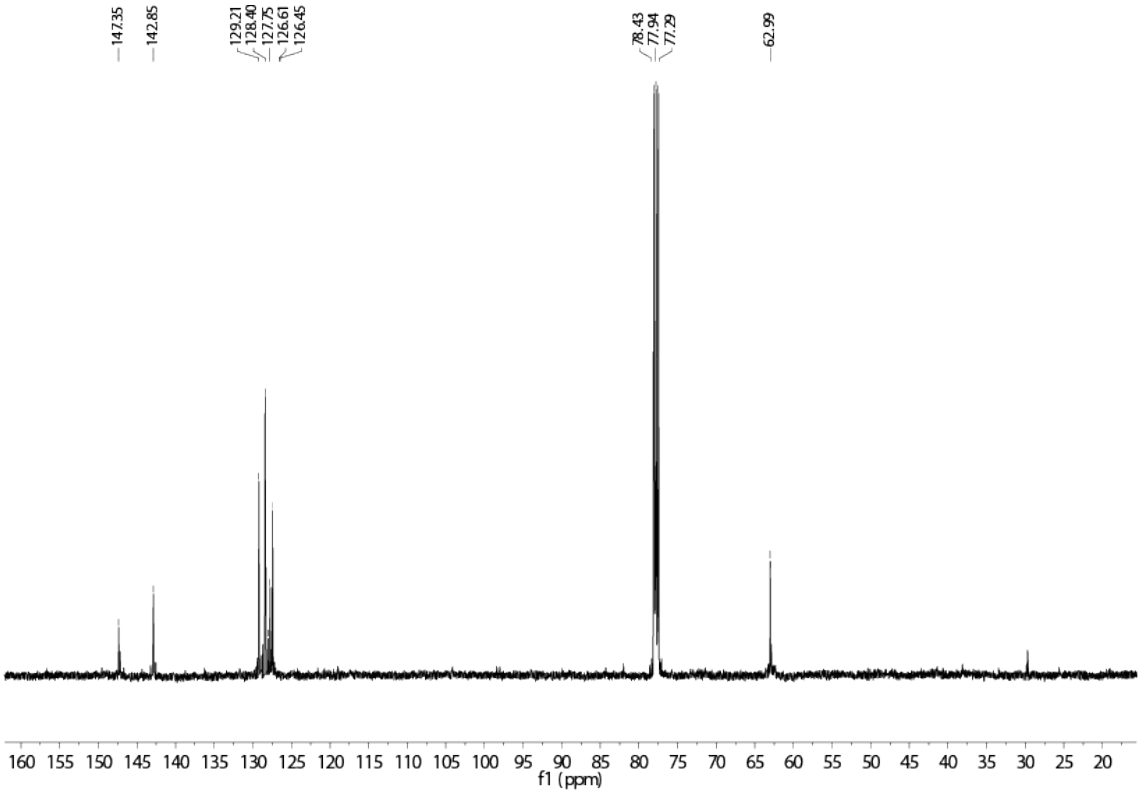

Figure S8. 8 - ^{13}C-NMR (100MHz, $CDCl_3$, 298K) Compound 4

Compound 5: Dibenzylamine[10]

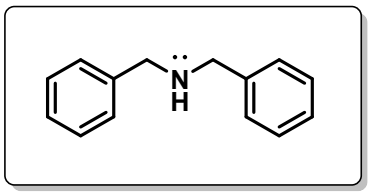

Yield: 91% (Yellow Oil)

^{1}H-NMR (400 MHz, $CDCl_3$) δ: 7.46-7.33 (8H, m), 7.32-7.26 (2H, m), 3.86 (4H, m), 1.93 (1H, bs)

^{13}C-NMR (100 MHz, $CDCl_3$) δ: 139.2, 129.6, 129.1, 128.6, 50.2

MS(ESI): m/z calcd. for $C_{14}H_{15}N$: 197.12, found $[M+H]^+$: 198.28

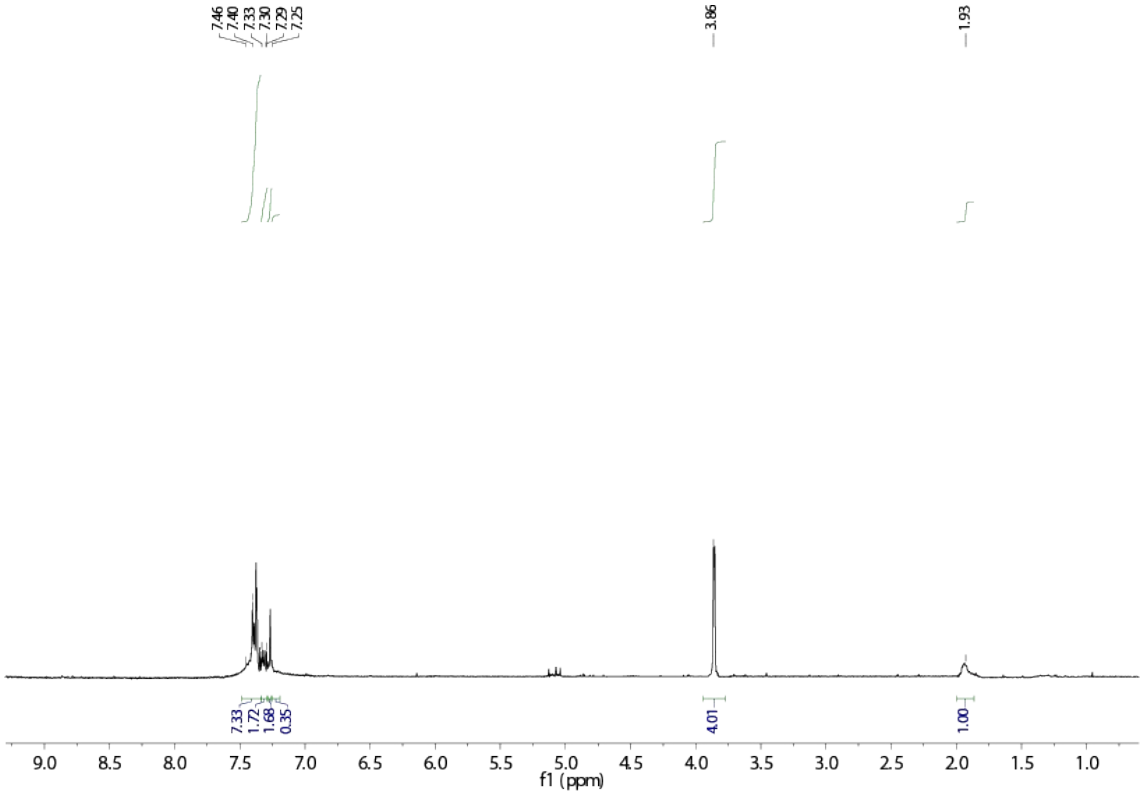

Figure S8.9 ^{1}H-NMR (400MHz, $CDCl_3$, 298K) Compound 5

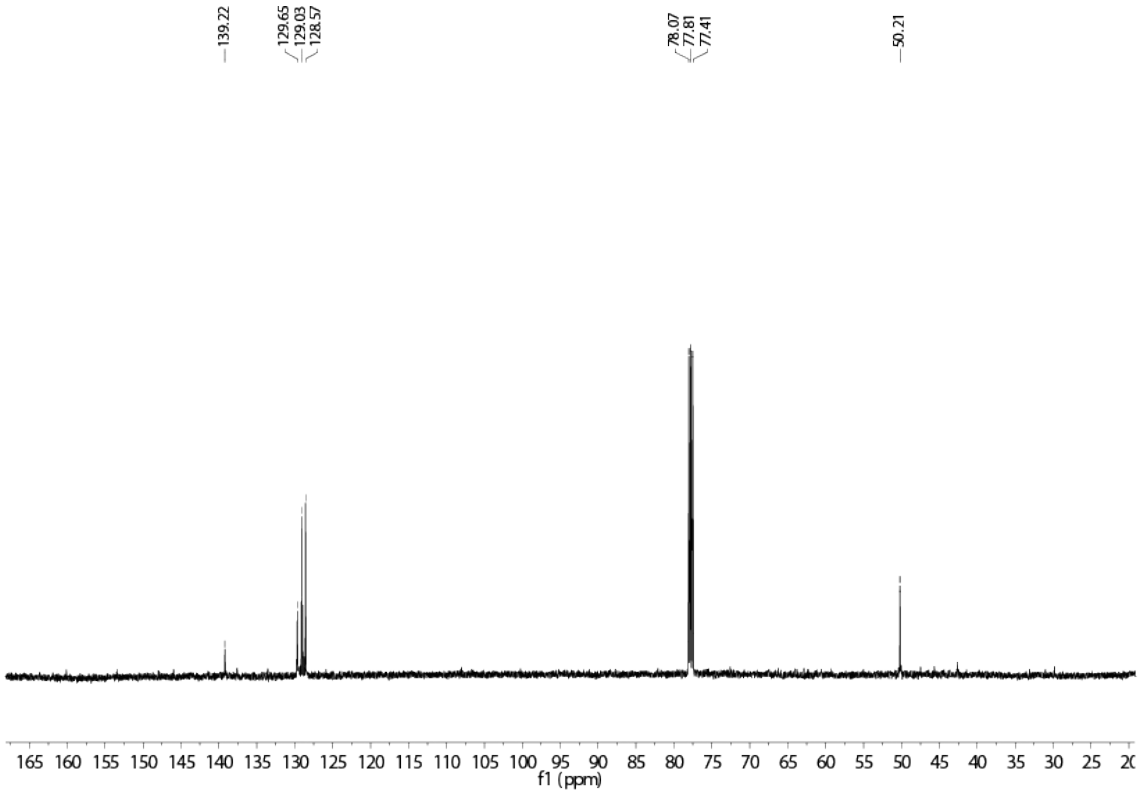

Figure S8. 10 - ^{13}C-NMR (100MHz, $CDCl_3$, 298K) Compound 5

Compound 6: N-benzyl-1,1-diphenylmethanamine[11]

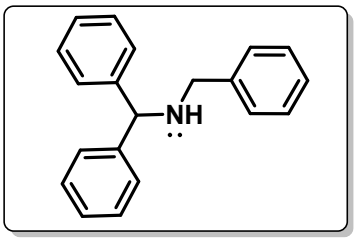

Yield: 96% (Yellow Solid)

^{1}H-NMR (400 MHz, $CDCl_3$) δ: 7.44 (4H, d, J=7.1 Hz), 7.39-7.31 (8H, m), 7.29-7.20 (4H, m), 4.89 (1H, s), 3.78 (2H, s), 2.27 (1H, bs)

^{13}C-NMR (100 MHz, $CDCl_3$) δ: 143.7, 140.4, 128.5, 127.6, 127.4, 126.5, 126.2, 64.7, 45.8

MS(ESI): m/z calcd. for $C_{20}H_{19}N$: 273.15, found $[M+H]^+$: 274.18

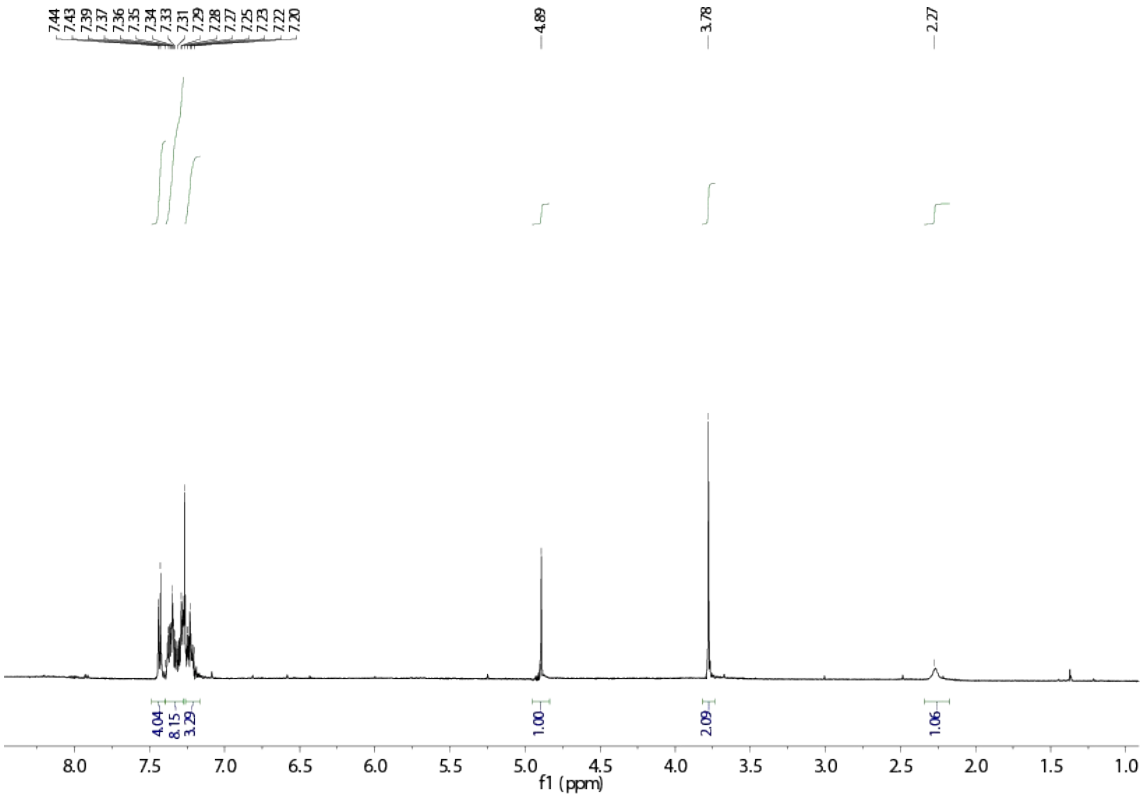

Figure S8.11 ^{1}H-NMR (400MHz, $CDCl_3$, 298K) Compound 6

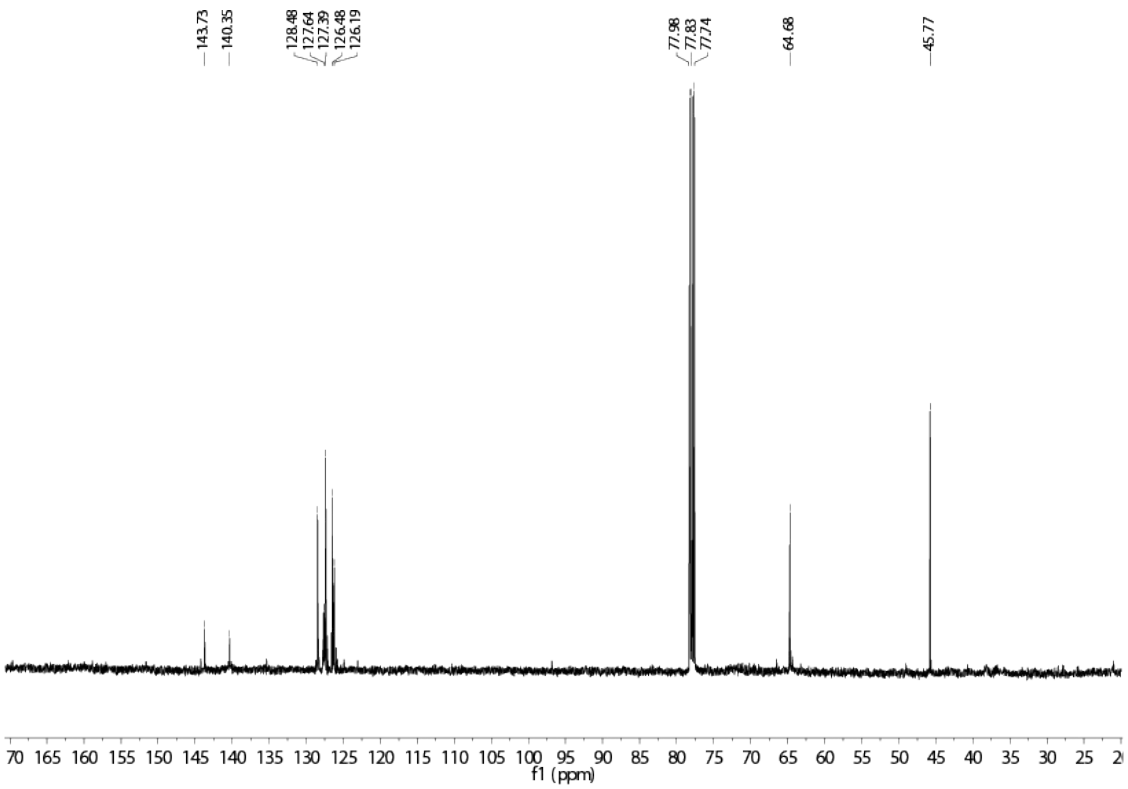

Figure S8. 12 - ^{13}C-NMR (100MHz, $CDCl_3$, 298K) Compound 6

Compound (4i): N,1,1-triphenylmethanimine[12]

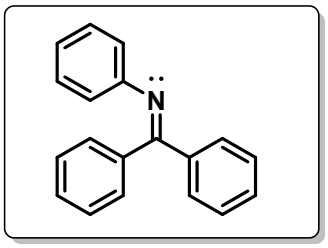

Yield: 95% (White Solid)

^{1}H-NMR (400 MHz, $CDCl_3$) δ: 7.68 (2H, dt, *J= 1.9, 7.9 Hz*), 7.39 (1H, tt, *J=1.5, 7.2 Hz*), 7.31 (2H, t, *J=7.5 Hz*), 7.20-7.14 (3H, m), 7.07-7.01 (4H, m), 6.83 (1H, tt, *J=1.1, 7.2 Hz*), 6.63 (2H, dd, *J=1.1, 8.3 Hz*)

^{13}C-NMR (100 MHz, $CDCl_3$) δ: 168.2, 151.3, 139.9, 136.1, 130.8, 129.9, 129.7, 129.2, 128.5, 128.1, 127.2, 124.0, 120.8

MS(ESI): m/z calcd. for $C_{19}H_{15}N$: 257.12, found: 257.10

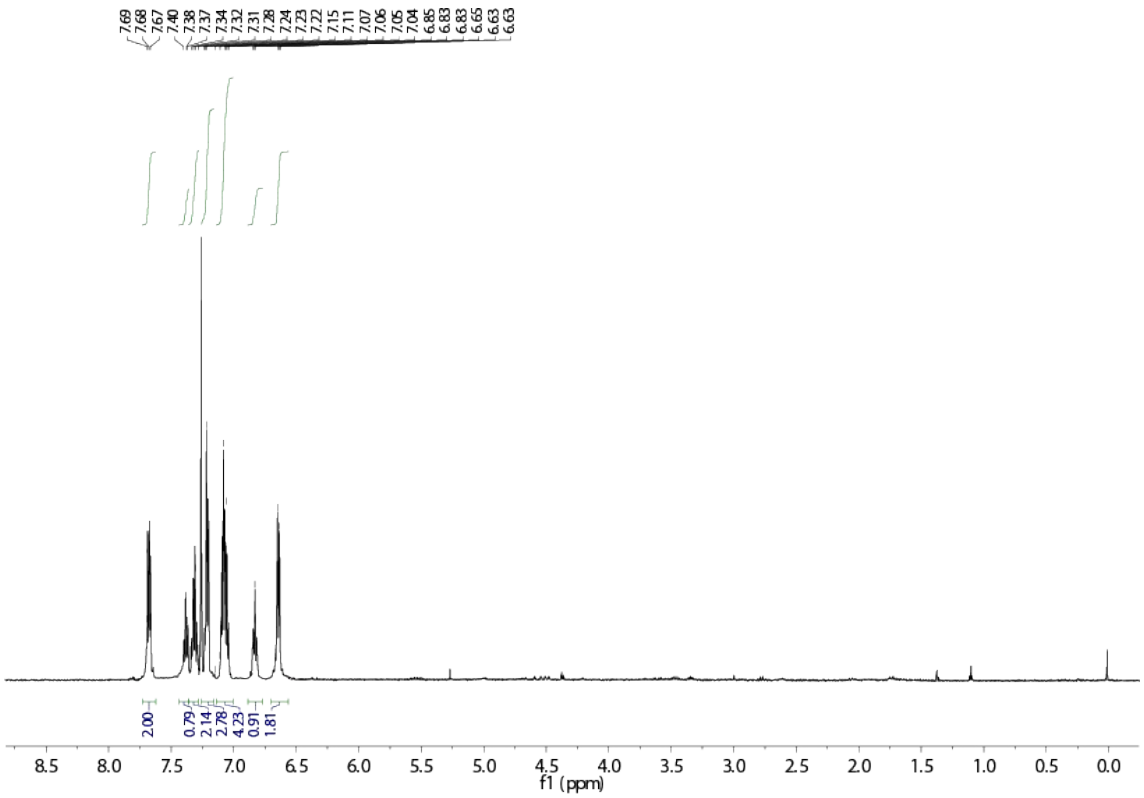

Figure S8.13 ^{1}H-NMR (400MHz, $CDCl_3$, 298K) Compound 4i

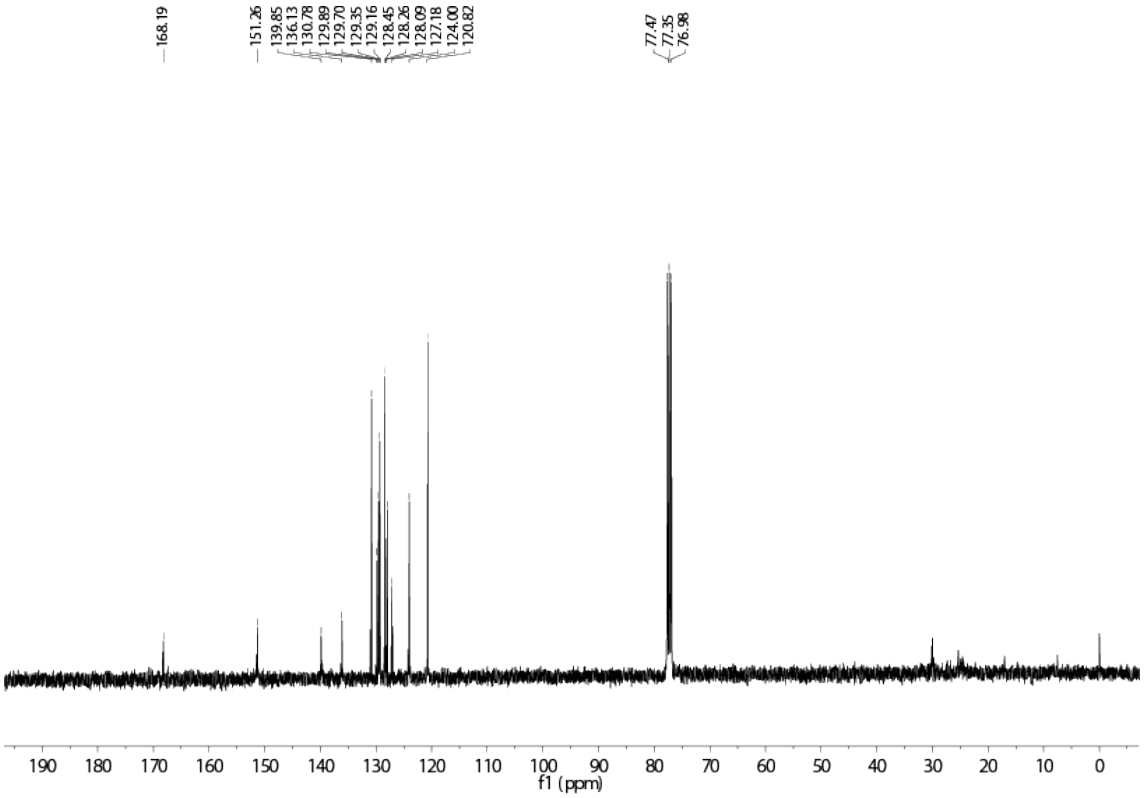

Figure S8. 14 - ^{13}C-NMR (100MHz, $CDCl_3$, 298K) Compound 4i

Compound (6i): N-benzyl-1,1-diphenylmethanimine[13]

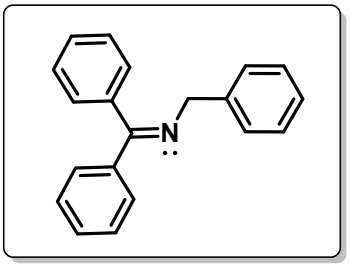

Yield: 96% (Colorless Solid)

^{1}H-NMR (400 MHz, $CDCl_3$) δ: 7.69-7.20 (15H, m), 4.61 (2H, m)

^{13}C-NMR (100 MHz, $CDCl_3$) δ: 169.9, 140.8, 139.9, 136.9, 130.2, 128.7, 128.4, 128.2, 127.5, 126.4, 57.3

MS(ESI): m/z calcd. for $C_{20}H_{18}N$: 272.14, found: 272.71.

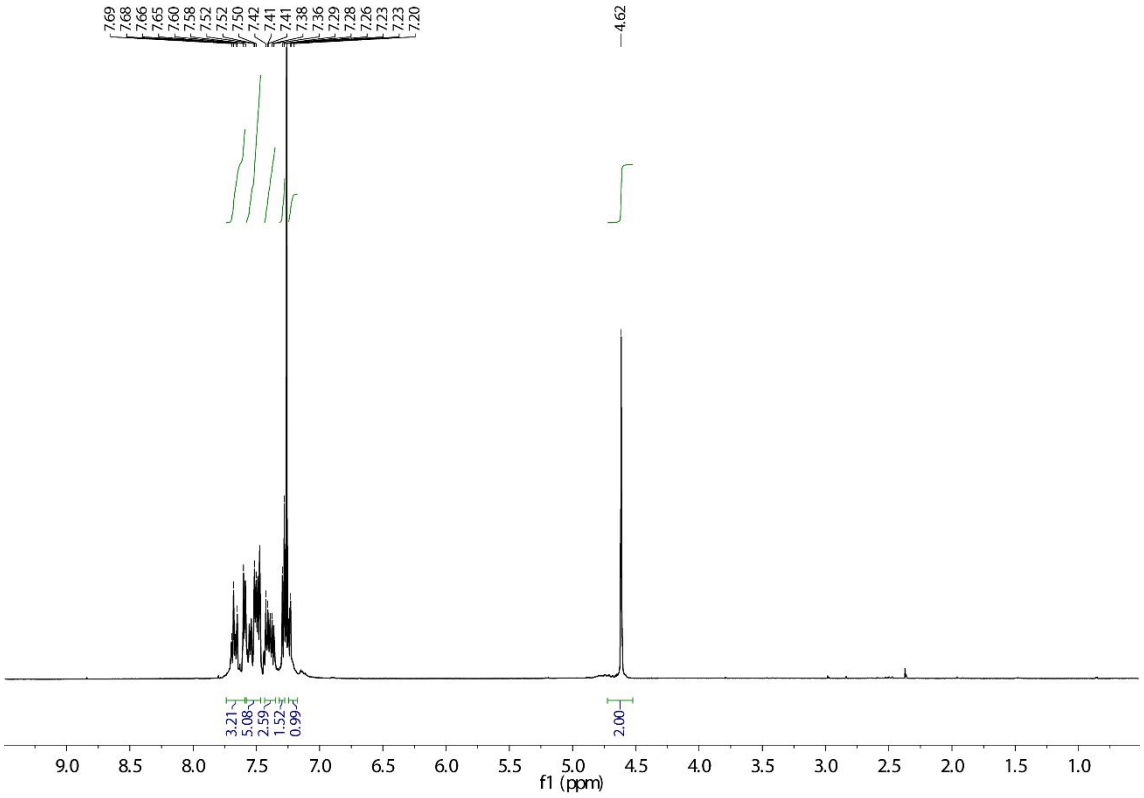

Figure S8.15 ^{1}H-NMR (400MHz, $CDCl_3$, 298K) Compound 6i

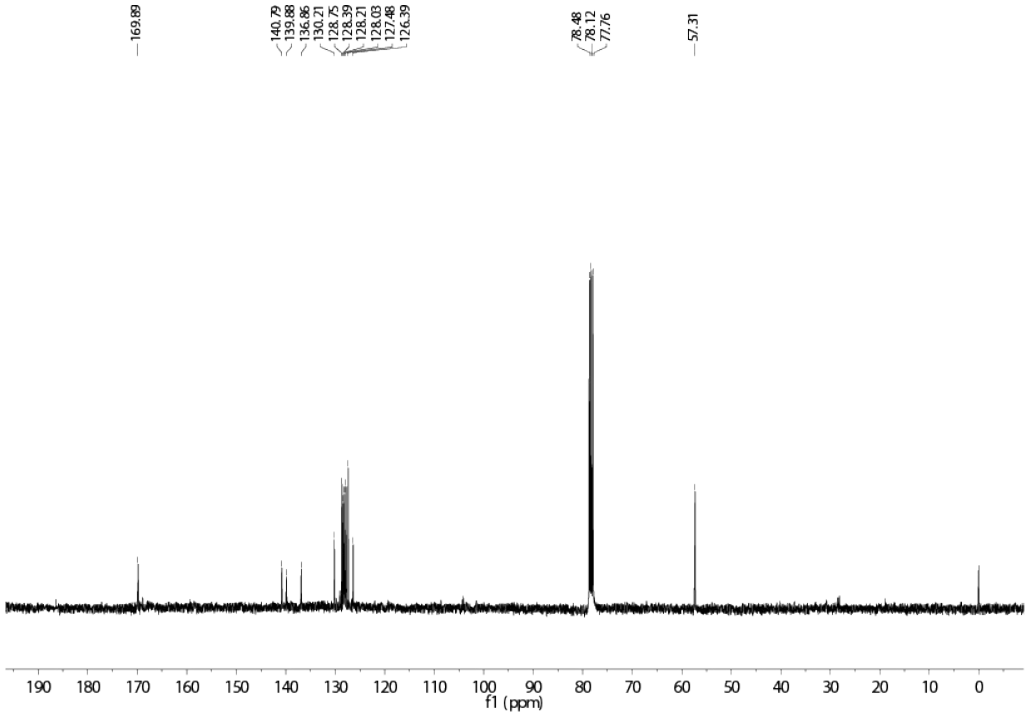

Figure S8. 16 - ^{13}C-NMR (100MHz, $CDCl_3$, 298K) Compound 6i

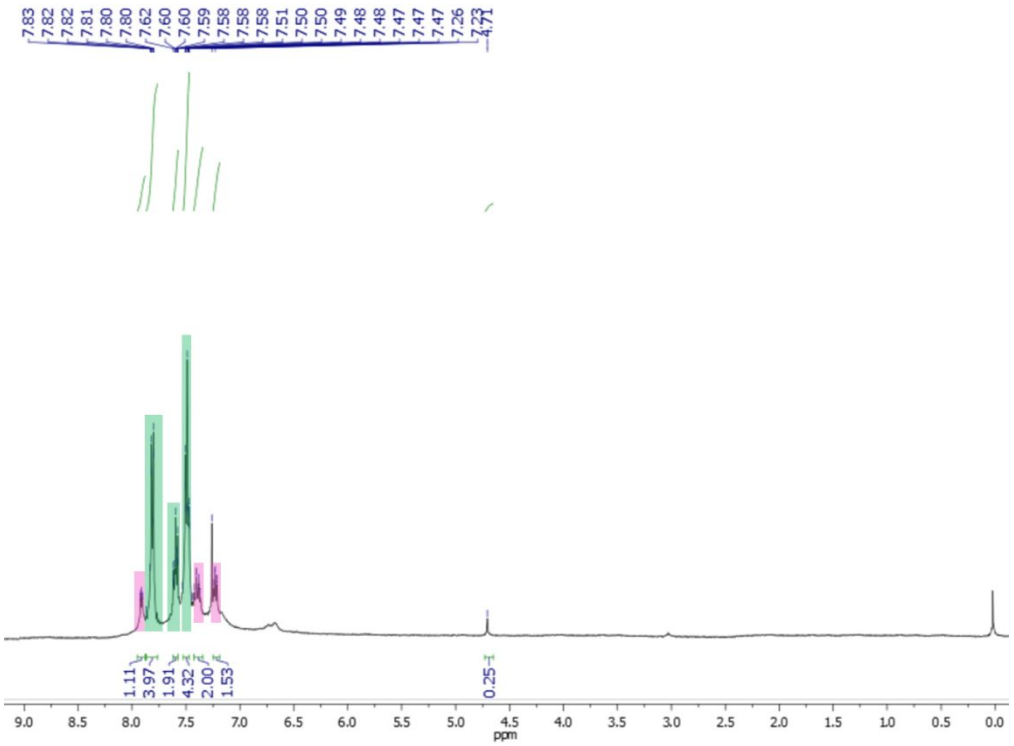

Figure S8. 17 ^{1}H-NMR (400MHz, $CDCl_3$, 298K) Reaction mixture using $Ni(NO_3)_2.6H_2O$ as catalyst

The crude of the reaction was analyzed by 1H-NMR, observing that the characteristic –CH– and –NH– signals at 5.58 and 4.28 ppm of the N-benzydrylaniline compound were not presented when Nickel precursor is used as catalyst. Unlike, the signals of the starting materials were clearly identified, being the green peaks the ones corresponding to benzophenone and the pink signals the ones from phenylamine.

9. Recovery and reusability test

After completion of the first run, Ni-URJC-4 catalyst was separated from the reaction mixture by simple filtration, washed with toluene, and dried up to 100 ° C under vacuum for 6 h. The recovered material was then reused as catalyst in further transformation under the standard conditions. Experimental results indicate that the catalyst could be recovered and reused without a significant deactivation in catalytic activity, since the yields are maintained practically identical after 2 runs. By comparing the XRD of Ni-URJC-4 before and after 2 reaction cycles, it is found that there are no obvious differences, which indicates that the crystallinity and structure can be kept well during the course of the reaction.

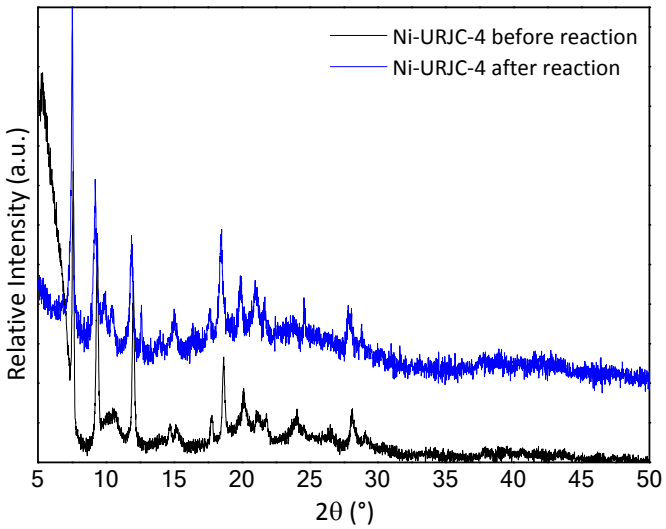

Figure S9.1 XRD patterns of the Ni-URJC-4 catalyst before and after reaction

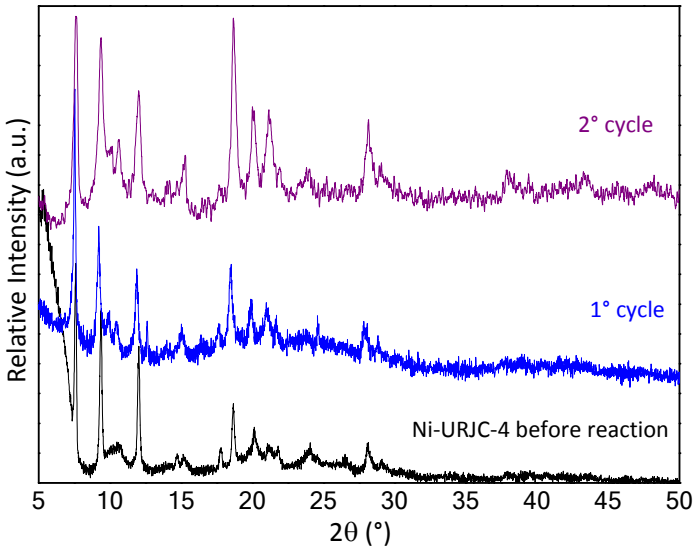

Figure S9.2. XRD patterns of the Ni-URJC-4 catalyst after two consecutive reactions

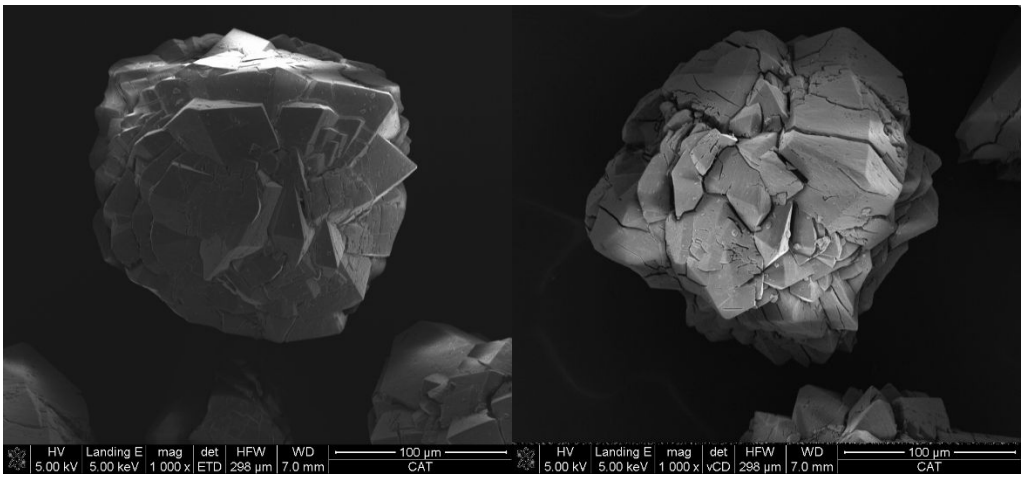

Figure S9.3. SEM images of pristine Ni-URJC-4 catalyst before reaction

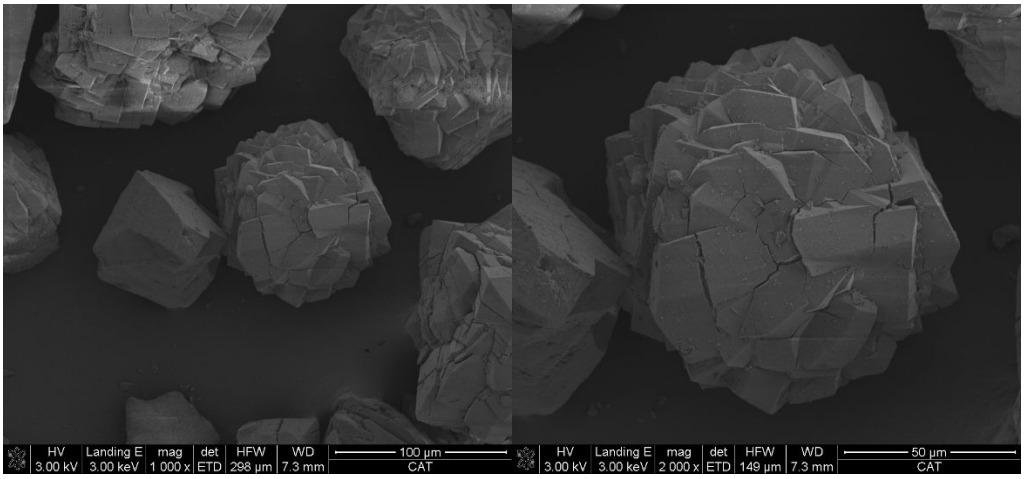

Figure S9.4. SEM images of Ni-URJC-4 catalyst after 1st reaction cycle

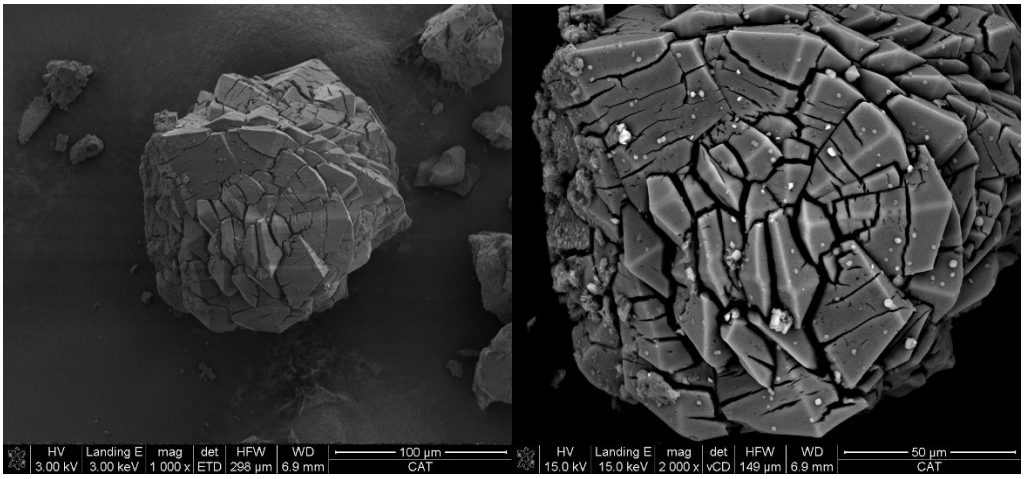

Figure S9.5. SEM images of Ni-URJC-4 catalyst after 2nd reaction cycle

References

[1] Bruker Apex2, Bruker AXS Inc., Madison, Wisconsin, USA, 2004.

[2] Krause, L.; Herbst-Irmer, R.; Sheldrick, G. M.; Stalke, D. Comparison of silver and molybdenum microfocus X-ray sources for single-crystal structure determination. J. Appl. Cryst. 2015, 48, 3-10.

[3] a) Sheldrick. G. M. SHELXT: Integrating space group determination and structure solution. Acta Cryst. 2015, 71, 3-8. b) Sheldrick, G. M. SHELX-2014, Program for Crystal Structure Refinement; University of Göttingen, Göttingen, Germany, 2014. (cb) Farrugia, L. J. WinGX suite for small molecule single-crystal crystallography. J. Appl. Cryst. 1999, 32, 837-838. (dc) Dolomanov, O. V.; Bourhis, L.J.; Gildea, R. J.; Howard, J. A. K.; Puschmann. H. OLEX2: a complete structure solution, refinement and analysis program. J. Appl. Cryst. 2009, 42, 339-341.

[4] Dolomanov, O. V.; Bourhis, L. J.; Gildea, R. J.; Howard, J. A. K.; Puschmann, H. OLEX2: a complete structure solution, refinement and analysis program. J. Appl. Crystallogr., 2009, 42, 339-341.

[5] Spek, A. L. Single-crystal structure validation with the program PLATON. J. Appl. Cryst., 2003, 36, 7-11.

[6] García-Ruano, J.L.; Parra, A.; Alemán, J.; Yuste, F.; Mastranzo, V. M. Monoalkylation of primary amines and N-sulfinylamides. *Chem. Commun*., **2009**, 404-406.

[7] Che, J.; Lam, Y. Polymer-Supported Hantzsch 1,4-Dihydropyridine Ester: An Efficient Biomimetic Hydrogen Source for the Reduction of Ketimines and Electron-Withdrawing Group Conjugated Olefins. *Adv. Synth. Catal*. **2010**, 352, 1752-1758.

[8] Muñoz, A.; Leo, P.; Orcajo, G.; Martinez, F.; Calleja, G. URJC-1-MOF as New Heterogeneous Recyclable Catalyst for C-Heteroatom Coupling Reactions. *ChemCatChem*, **2019**, 11, 3376-3380.

[9] Subaramanian, M.; Midya, S. P.; Ramar, P. M.; Balaraman, E. General Synthesis of N-Alkylation of Amines with Secondary Alcohols via Hydrogen Autotransfer. *Org. Lett*., **2019**, 21, 8899-8903.

[10] Corre, Y.; Trivelli X.; Capet, F.; Djukic, J.P.; Agbossou-Niedercorn, F.; Michon, C. Efficient and Selective Hydrosilylation of Secondary and Tertiary Amides Catalyzed by an Iridium(III) Metallacycle: Development and Mechanistic Investigation. *ChemCatChem,* **2017**, 9, 2009-2017.

[11] Zheng, N.; Weijie Z.; Pui C. L.; Aguila B.; Ma S. Promoting Frustrated Lewis Pairs for Heterogeneous Chemoselective Hydrogenation via the Tailored Pore Environment within Metal–Organic Frameworks. *Angew. Chem. Int. Ed.* **2019***, 58,* 7420-7424.

[12] Ogata, T.; Hartwig, J. F. Palladium-Catalyzed Amination of Aryl and Heteroaryl Tosylates at Room Temperature. *J. Am. Chem. Soc*. **2008**, 130, 42, 13848-13849.

[13] Koyama, Y.; Gudeangadi, P. G. One-pot synthesis of alternating peptides exploiting a new polymerization technique based on Ugi's 4CC reaction. *Chem. Commun*., **2017**, 53, 3846-3849.